

Table 1  
Effects of G-CSF on complete blood count, coagulation time, and biochemical parameters in WHHL-MI rabbits

	WBC (/mm <sup>3</sup> )	RBC (×10 <sup>4</sup> /mm <sup>3</sup> )	Plt (×10 <sup>4</sup> /mm <sup>3</sup> )	APTT (s)	PT (s)	TC (mg/dl)	LDL-C (mg/dl)	TG (mg/dl)
Control (n = 7)								
Pretreatment	8300 ± 240	658 ± 106	41.5 ± 12.6	62.3 ± 24.2	9.6 ± 2.6	509 ± 102	423 ± 102	46 ± 12
1 week	10,300 ± 1240	634 ± 133	48.6 ± 18.6	72.5 ± 25.6	10.1 ± 1.9	530 ± 87	445 ± 77	53 ± 9
4 weeks	9200 ± 580	632 ± 133	52.3 ± 19.5	89.3 ± 36.3	8.9 ± 3.2	527 ± 76	420 ± 80	49 ± 11
G-CSF (n = 7)								
Pretreatment	8300 ± 240	658 ± 113	52.3 ± 19.8	89.6 ± 25.2	10.2 ± 2.1	598 ± 133	417 ± 144	50 ± 15
1 week	41,600 ± 8450 <sup>a</sup>	685 ± 103	49.5 ± 24.2	104.2 ± 56.3	8.5 ± 2.7	579 ± 116	432 ± 117	47 ± 14
4 weeks	9400 ± 680	690 ± 156	56.6 ± 28.5	78.5 ± 45.3	8.1 ± 2.3	521 ± 266	450 ± 96	62 ± 13

Results are expressed as means ± SEM.

<sup>a</sup> P < 0.05 vs control group.

Table 2  
Effects of G-CSF on complete blood count, coagulation time, and biochemical parameters in balloon injury model

	WBC (/mm <sup>3</sup> )	RBC (×10 <sup>4</sup> /mm <sup>3</sup> )	Plt (×10 <sup>4</sup> /mm <sup>3</sup> )	APTT (s)	PT (s)	TC (mg/dl)	LDL-C (mg/dl)	TG (mg/dl)
Control (n = 10)								
Preoperation	11,300 ± 1700	623 ± 103	51.0 ± 19.5	55.6 ± 35.3	12.6 ± 10.8	951 ± 467	392 ± 164	40 ± 59
1 week	26,800 ± 9400 <sup>a</sup>	538 ± 126	62.2 ± 20.5	74.0 ± 33.7	8.1 ± 1.9	1699 ± 587	637 ± 147	74 ± 33
4 weeks	14,400 ± 3600	609 ± 98	53.5 ± 11.8	140.0 ± 56.8	9.0 ± 2.7	2435 ± 990	735 ± 279	111 ± 99
G-CSF (n = 10)								
Preoperation	8900 ± 1600	598 ± 98	60.2 ± 21.1	131.2 ± 35.3	9.0 ± 1.1	1193 ± 420	385 ± 100	28 ± 4
1 week	66,800 ± 23,600 <sup>a,b</sup>	485 ± 83	36.3 ± 20.7	104.7 ± 30.3	7.5 ± 1.6	1951 ± 315	715 ± 384	104 ± 41
4 weeks	10,100 ± 200	586 ± 93	47.9 ± 18.5	61.3 ± 36.3	8.1 ± 0.1	2275 ± 234	593 ± 110	184 ± 86

Results are expressed as means ± SEM.

<sup>a</sup> P < 0.05 vs preoperation.

<sup>b</sup> P < 0.05 vs control group.

WBC in this model was similar to that in human treated with 10 µg/kg/day of G-CSF.

In balloon injury model, there were no significant differences in serum levels of TC, LDL-C, and TG between control group and G-CSF group (Table 2). There were also no significant differences in APTT and PT between control group and G-CSF group in both models. The numbers of RBC and Plt were not different between two groups. The number of WBC was increased at 7 days after treatment in control group (1 week, 26,800 ± 9400/mm<sup>3</sup> vs preoperation, 11,300 ± 1700/mm<sup>3</sup>, P < 0.05) and in G-CSF group (1 week, 66,800 ± 23,600/mm<sup>3</sup> vs preoperation, 8900 ± 1600/mm<sup>3</sup>, P < 0.05) (Table 2).

#### Effects of G-CSF on coronary atherosclerotic lesions in WHHL-MI rabbits

To investigate the effect of G-CSF on the progression of the atherosclerosis of coronary artery in WHHL-MI rabbit, we examined the coronary artery and the thoracic aorta. Fig. 1 shows the coronary stenosis in G-CSF group and control group of WHHL-MI rabbits. There was a marked difference in the stenosis score of all coronary arteries including RCA, LAD, and LCX of WHHL-MI rabbits between the G-CSF group and control group (Figs. 1A and B). The coronary stenosis score of the G-CSF group was much lower (8.9 ± 7.0) than that of control group (22.6 ± 8.0) in LCX (Fig. 1B). Since the stenosis of LCX was more prominent

among three coronary arteries in this model [18], we examined the composition of smooth muscle cells, macrophages, extracellular lipid deposits and collagen in the coronary atherosclerotic lesion of the LCX in the presence or absence of G-CSF treatment. There was no significant difference in the percent area of each composition in the plaque between G-CSF group and control group (G-CSF group: smooth muscle cells, 40.4 ± 11.2%; macrophages, 11.4 ± 8.9%; extracellular lipid deposits, 4.4 ± 4.7%; collagen, 39.2 ± 10.9%, control group: smooth muscle cells, 45.3 ± 14.4%; macrophages, 13.5 ± 9.3%; extracellular lipid deposits, 6.5 ± 4.7%; collagen, 38.3 ± 2.2%) (Fig. 1C). The average of the most severe stenosis of G-CSF group was significantly low (48.5 ± 28.5%) compared with that of control group (72.7 ± 24.5%) in LCX. The area of lipid plaque detected by Sudan IV staining of thoracic aorta was significantly smaller in G-CSF group than control group (G-CSF group, 34.4 ± 18.0% vs control group, 49.6 ± 22.2%, P < 0.05) (Figs. 2A and B).

It has been reported that intraplaque neovascularization facilitates the progression and rupture of plaque [21]. Although we previously reported that G-CSF prevents LV remodeling and dysfunction after AMI through neovascularization in the ischemic region, G-CSF did not induce neovascularization in atherosclerotic plaque of WHHL-MI rabbits (data not shown). The treatment with G-CSF inhibited the progression of atherosclerosis in coronary artery and aorta at 4 weeks after the treatment. The role of G-CSF on

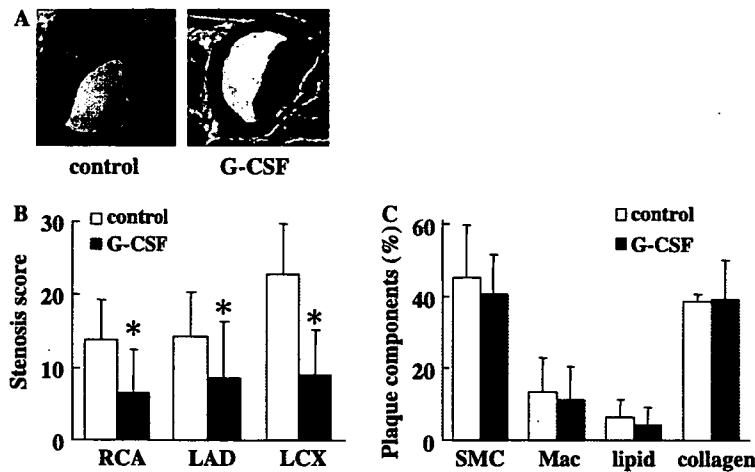


Fig. 1. Effects of G-CSF on the coronary atherosclerosis of WHHL-MI rabbits. The representative atherosclerotic lesion in LCX (A), coronary stenosis score (B), and plaque components (C) in WHHL-MI rabbits.  $n = 7$  in each group. RCA, right coronary artery; LAD, left anterior descending artery; LCX, left circumflex artery; SMC, smooth muscle cells; Mac, macrophages. Results are expressed as means  $\pm$  SEM. Scale bars indicate 200  $\mu$ m. \* $P < 0.05$  vs control.

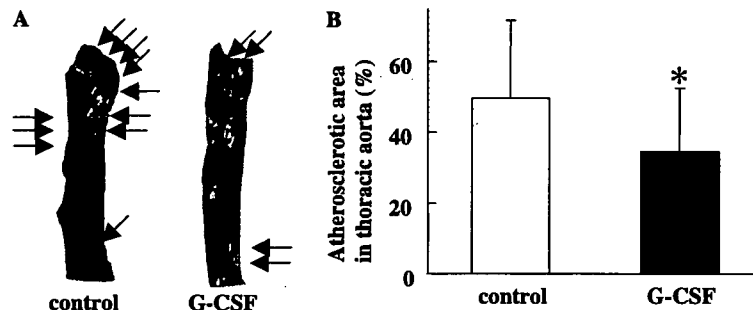


Fig. 2. Effects of G-CSF on the atherosclerosis of aorta of WHHL-MI rabbits. The representative atherosclerotic lesion of aorta (A) and the ratio of atherosclerotic area to thoracic aorta area in WHHL-MI rabbits (B). Arrows indicate atherosclerotic lesions. Results are expressed as means  $\pm$  SEM.  $n = 7$  in each group. \* $P < 0.05$  vs control.

coronary atherosclerosis is thought to be the prevention of the progression of atherosclerosis but not the regression since age-dependent atherosclerotic change would be very progressive during 14–15 months old (coronary stenosis score at 14 months old: RCA,  $6.8 \pm 6.8$ ; LAD,  $7.0 \pm 6.7$ ; LCX,  $7.8 \pm 5.4$ ;  $n = 4$ ). Since the persistent inflammatory response has been reported to be involved in the progression of atherosclerosis [22–24], the anti-inflammatory effect [1,25] of G-CSF may block the vicious circle of the progression of atherosclerosis in those models. There was no significant difference in the percent area of smooth muscle cells, macrophages, extracellular lipid deposits, and collagen in the plaque between G-CSF group and control group. It remains to be determined how G-CSF prevents the progression of atherosclerosis in WHHL-MI rabbits.

#### Effects of G-CSF on neointimal formation after vascular injury and reendothelialization in balloon injured rabbit artery

The restenosis after balloon angioplasty is mainly caused by neointimal hyperplasia. In our balloon injury

model, neointima volume of injured arteries after 4 weeks was significantly higher than that of contralateral artery (Fig. 3B). The treatment with G-CSF strongly prevented the neointimal formation in injured arteries compared with control group (G-CSF group,  $0.56 \pm 0.14$  mm<sup>2</sup> vs control group,  $0.84 \pm 0.13$  mm<sup>2</sup>,  $P < 0.05$ ) (Figs. 3A and B). The neointima/media ratio was significantly smaller in G-CSF group than control group (G-CSF group,  $0.91 \pm 0.22$  vs control group,  $1.24 \pm 0.21$ ,  $P < 0.05$ ) (Fig. 3C).

The treatment with G-CSF did not influence the infiltration of macrophages in the plaque area of balloon injury (1 week; G-CSF group,  $3.8 \pm 0.6\%$  vs control group,  $3.5 \pm 0.5\%$ , 4 weeks; G-CSF group,  $5.1 \pm 1.1\%$  vs control group,  $6.7 \pm 1.1\%$ ) (Figs. 3D and E). The number of infiltrated neutrophils at 1 week was more observed in G-CSF group than control group (G-CSF group,  $0.18 \pm 0.04\%$  vs control group,  $0.01 \pm 0.01\%$ ,  $P < 0.05$ ), although there was no difference in infiltration of neutrophils in the plaque area between two groups at 4 weeks (Fig. 3F).

The ratio of reendothelialization was significantly accelerated by the treatment with G-CSF at both 1 week and 4 weeks (1 week; G-CSF group,  $62.8 \pm 2.2\%$  vs control

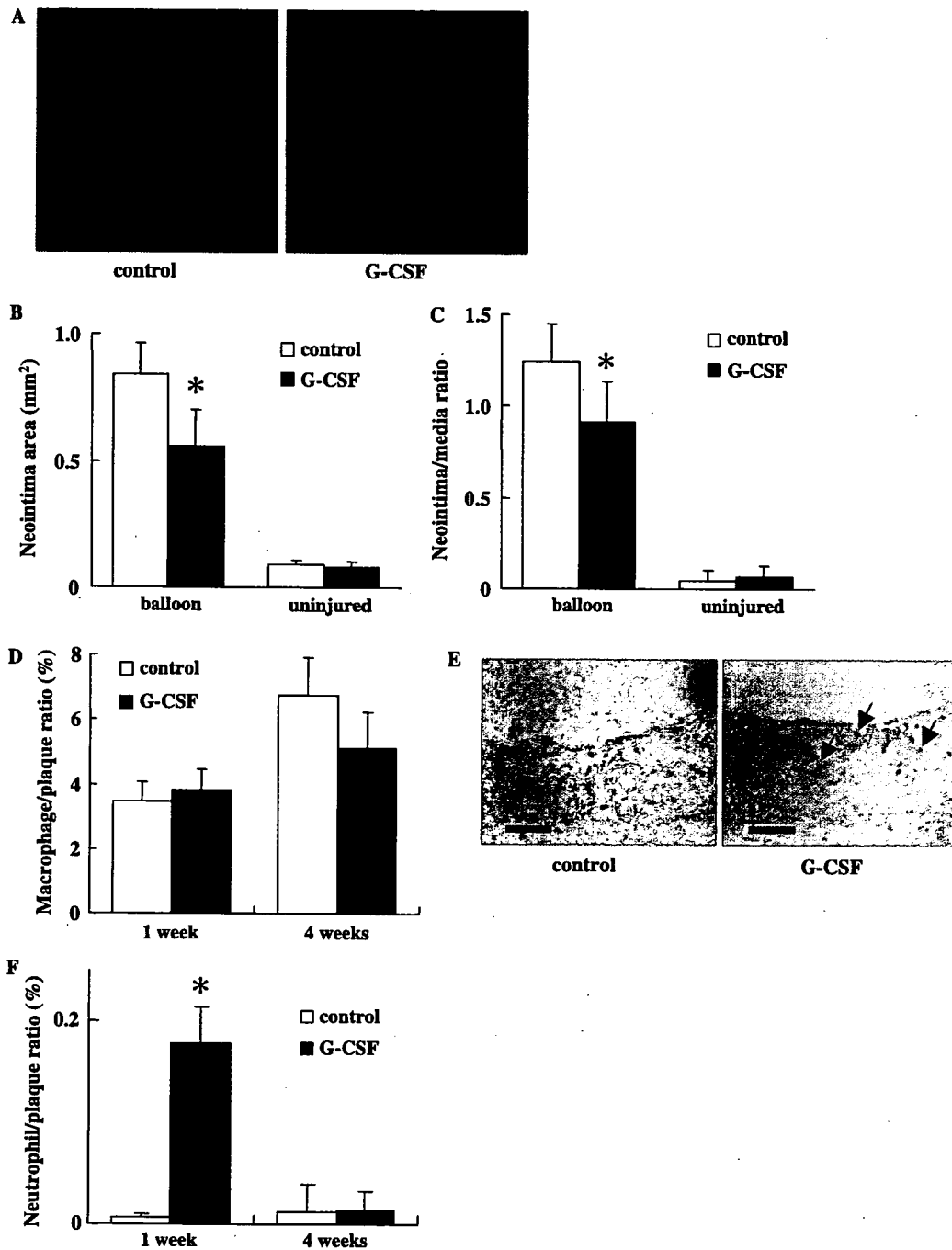


Fig. 3. Effects of G-CSF on the atherosclerosis of balloon injured artery. The representative balloon injury-induced neointimal formation (A), neointima area (B), and neointima/media ratio of rabbit iliac arteries (C) at 4 weeks ( $n = 10$  in each group). The percentage of infiltrated macrophages at 1 week ( $n = 5$  in each group) and 4 weeks ( $n = 10$  in each group) (D) after balloon injury in rabbit iliac arteries. The representative photograph of neutrophils infiltrated in neointima of control rabbit and G-CSF-treated rabbit (E). The percentage of infiltrated neutrophils at 1 week after balloon injury in rabbit iliac artery (F). Arrows indicate the infiltrated neutrophils. Scale bars indicate 50  $\mu\text{m}$ . Results are expressed as means  $\pm$  SEM. \* $P < 0.05$  vs control.

group,  $46.7 \pm 2.9\%$ ,  $P < 0.05$ , 4 weeks; G-CSF group,  $79.6 \pm 3.7\%$  vs control group,  $58.9 \pm 8.5\%$ ,  $P < 0.05$ ) (Figs. 4A and B). The pretreatment with L-NAME significantly inhibited G-CSF-induced reendothelialization (G-CSF group,  $41.8 \pm 9.1\%$  vs control group,  $36.5 \pm 7.6\%$ ) (Fig. 4B).

These results suggest that G-CSF also prevented the progression of the neointimal formation in rabbit vascular injury model. Vascular injury-induced denudation of endothelial cells (ECs) leads to elevated vascular tone, migration and infiltration of smooth muscle cells and activation of cytokine network, resulting in the

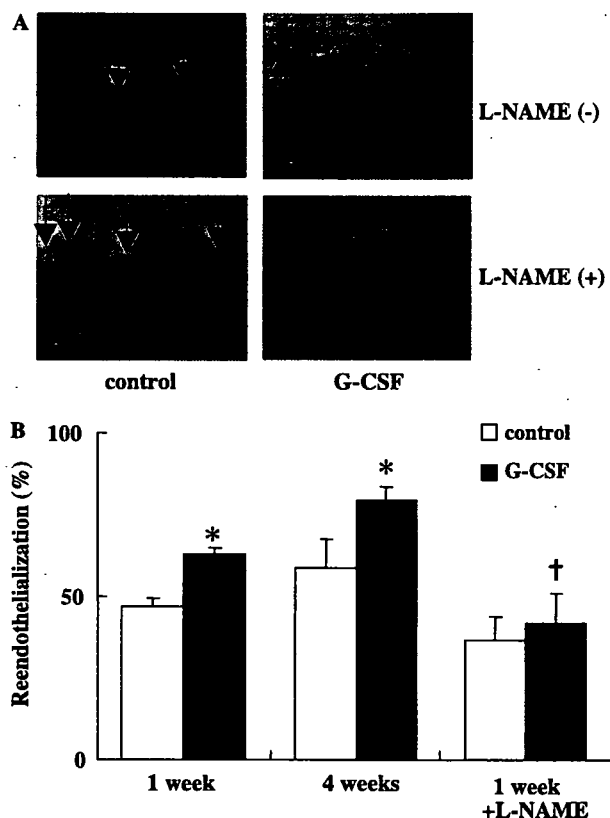


Fig. 4. Effects of G-CSF on reendothelialization. (A) The representative photographs of CD31-positive cells in injured arteries at 1 week after balloon injury in the absence or presence of L-NAME ( $n = 5$  in each group). Arrows indicate the absence region of endothelium. Scale bars indicate 100  $\mu\text{m}$ . (B) The percentage of CD31-positive cell coverage in injured arteries at 1 and 4 weeks after balloon injury. Results are expressed as means  $\pm$  SEM. \* $P < 0.05$  vs control. † $P < 0.05$  vs G-CSF group at 1 week without pretreatment with L-NAME.

neointimal formation [15]. EPCs have been recently reported to enhance reendothelialization and reduce neointimal formation after carotid artery injury in mice and rabbits [26,27]. G-CSF treatment has been reported to increase the number of circulating EPCs [28]. Since nitric oxide plays a critical role in the mobilization of EPCs from bone marrow [29,30], we examined using a NOS inhibitor, L-NAME, whether the mobilization of EPCs is involved in the G-CSF-induced reendothelialization. The pretreatment with L-NAME significantly inhibited the G-CSF-induced reendothelialization in balloon injured artery, suggesting that the recruitment and mobilization of EPCs from bone marrow are involved in the beneficial effects of G-CSF on balloon-injured stenosis. The other mechanisms including anti-inflammatory effect, anti-apoptotic effect, and modification of extracellular matrix may be also involved in the effects of G-CSF. Recent clinical studies have reported that G-CSF therapy does not induce the progression of atherosclerosis in the patients with coronary artery disease [31–35].

## Concluding remarks

In the present study, we demonstrated using two kinds of rabbit models of atherosclerosis that the treatment with G-CSF ameliorates the progression of atherosclerosis. The treatment with G-CSF inhibited the progression of atherosclerosis and neointimal formation. These results suggest that G-CSF has a therapeutic potential for the progression of atherosclerosis. Randomized clinical trials to evaluate the feasibility and safety of G-CSF on coronary artery diseases are warranted.

## Acknowledgments

We thank to Reiko Kobayashi, Emi Fujita, Megumi Ikeda, Akane Furuyama, and Yuko Ohtsuki for technical assistance. This work was supported by Health and Labour Sciences Research Grants, Takeda Medical Research Foundation, Uehara Memorial Foundation, Grant-in-Aid of The Japan Medical Association, The Kato Memorial Trust for Nambyo Research, and Takeda Science Foundation.

## References

- [1] D.W. Hommes, J. Meenan, S. Dijkhuizen, F.J. Ten Kate, G.N. Tytgat, S.J. Van Deventer, Efficacy of recombinant granulocyte colony-stimulating factor (rhG-CSF) in experimental colitis, *Clin. Exp. Immunol.* 106 (1996) 529–533.
- [2] D. Orlic, J. Kajstura, S. Chimenti, F. Limana, I. Jakoniuk, F. Quaini, B. Nadal-Ginard, D.M. Bodine, A. Leri, P. Anversa, Mobilized bone marrow cells repair the infarcted heart, improving function and survival, *Proc. Natl. Acad. Sci. USA* 98 (2001) 10344–10349.
- [3] M. Ohtsuka, H. Takano, Y. Zou, H. Toko, H. Akazawa, Y. Qin, M. Suzuki, H. Hasegawa, H. Nakaya, I. Komuro, Cytokine therapy prevents left ventricular remodeling and dysfunction after myocardial infarction through neovascularization, *FASEB J.* 18 (2004) 851–853.
- [4] K. Iwanaga, H. Takano, M. Ohtsuka, H. Hasegawa, Y. Zou, Y. Qin, K. Odaka, K. Hiroshima, H. Tadokoro, I. Komuro, Effects of G-CSF on cardiac remodeling after acute myocardial infarction in swine, *Biochem. Biophys. Res. Commun.* 325 (2004) 1353–1359.
- [5] S. Minatoguchi, G. Takemura, X.H. Chen, N. Wang, Y. Uno, M. Koda, M. Arai, Y. Misao, C. Lu, K. Suzuki, K. Goto, A. Komada, T. Takahashi, K. Kosai, T. Fujiwara, H. Fujiwara, Acceleration of the healing process and myocardial regeneration may be important as a mechanism of improvement of cardiac function and remodeling by postinfarction granulocyte colony-stimulating factor treatment, *Circulation* 109 (2004) 2572–2580.
- [6] M. Harada, Y. Qin, H. Takano, T. Minamino, Y. Zou, H. Toko, M. Ohtsuka, K. Matsuura, M. Sano, J. Nishi, K. Iwanaga, H. Akazawa, T. Kunieda, W. Zhu, H. Hasegawa, K. Kunisada, T. Nagai, H. Nakaya, K. Yamauchi-Takahara, I. Komuro, G-CSF prevents cardiac remodeling after myocardial infarction by activating the Jak-Stat pathway in cardiomyocytes, *Nat. Med.* 11 (2005) 305–311.
- [7] H. Hasegawa, H. Takano, K. Iwanaga, M. Ohtsuka, Y. Qin, Y. Niitsuma, K. Ueda, T. Toyoda, H. Tadokoro, I. Komuro, Cardio-protective effects of granulocyte colony-stimulating factor in chronic hibernating swine myocardium, *J. Am. Coll. Cardiol.* 47 (2006) 842–849.
- [8] H. Takano, M. Ohtsuka, H. Akazawa, H. Toko, M. Harada, H. Hasegawa, T. Nagai, I. Komuro, Pleiotropic effects of cytokines on acute myocardial infarction: G-CSF as a novel therapy for acute myocardial infarction, *Curr. Pharm. Des.* 9 (2003) 1121–1127.

- [9] H.J. Kang, H.S. Kim, S.Y. Zhang, K.W. Park, H.J. Cho, B.K. Koo, Y.J. Kim, D. Soo Lee, D.W. Sohn, K.S. Han, B.H. Oh, M.M. Lee, Y.B. Park, Effects of intracoronary infusion of peripheral blood stem-cells mobilised with granulocyte-colony stimulating factor on left ventricular systolic function and restenosis after coronary stenting in myocardial infarction: the MAGIC cell randomised clinical trial, *Lancet* 363 (2004) 751–756.
- [10] Y. Watanabe, Serial inbreeding of rabbits with hereditary hyperlipidemia (WHHL-rabbit), *Atherosclerosis* 36 (1980) 261–268.
- [11] M. Shiomi, T. Ito, Effect of cerivastatin sodium, a new inhibitor of HMG-CoA reductase, on plasma lipid levels, progression of atherosclerosis, and the lesional composition in the plaques of WHHL rabbits, *Br. J. Pharmacol.* 126 (1999) 961–968.
- [12] M. Shiomi, T. Ito, M. Shirashi, Y. Watanabe, Inheritability of atherosclerosis and the role of lipoproteins as risk factors in the development of atherosclerosis in WHHL rabbits: risk factors related to coronary atherosclerosis are different from those related to aortic atherosclerosis, *Atherosclerosis* 96 (1992) 43–52.
- [13] M. Shiomi, T. Ito, S. Yamada, S. Kawashima, J. Fan, Development of an animal model for spontaneous myocardial infarction (WHHLMI rabbit), *Arterioscler. Thromb. Vasc. Biol.* 23 (2003) 1239–1244.
- [14] S.L. Stevens, K. Hilgath, U.S. Ryan, J. Trachtenberg, E. Choi, A.D. Callow, The synergistic effect of hypercholesterolemia and mechanical injury on intimal hyperplasia, *Ann. Vasc. Surg.* 6 (1992) 655–661.
- [15] J.R. Wilentz, T.A. Sanborn, C.C. Haudenschild, C.R. Valeri, T.J. Ryan, D.P. Faxon, Platelet accumulation in experimental angioplasty: time course and relation to vascular injury, *Circulation* 75 (1987) 636–642.
- [16] N. Beohar, J.D. Flaherty, C.J. Davidson, R.C. Maynard, J.D. Robbins, A.P. Shah, J.W. Choi, L.A. MacDonald, J.P. Jorgensen, J.V. Pinto, S. Chandra, H.M. Klaus, N.C. Wang, K.R. Harris, R. Decker, R.O. Bonow, Antirestenotic effects of a locally delivered caspase inhibitor in a balloon injury model, *Circulation* 109 (2004) 108–113.
- [17] M. Shiomi, T. Ito, Y. Hirouchi, M. Enomoto, Fibromuscular cap composition is important for the stability of established atherosclerotic plaques in mature WHHL rabbits treated with statins, *Atherosclerosis* 157 (2001) 75–84.
- [18] K. Ishikawa, D. Sugawara, J. Goto, Y. Watanabe, K. Kawamura, M. Shiomi, H. Itabe, Y. Maruyama, Heme oxygenase-1 inhibits atherogenesis in Watanabe heritable hyperlipidemic rabbits, *Circulation* 104 (2001) 1831–1836.
- [19] M. Shiomi, T. Ito, T. Tsukada, T. Yata, Y. Watanabe, Y. Tsujita, M. Fukami, J. Fukushige, T. Hosokawa, A. Tamura, Reduction of serum cholesterol levels alters lesional composition of atherosclerotic plaques. Effect of pravastatin sodium on atherosclerosis in mature WHHL rabbits, *Arterioscler. Thromb. Vasc. Biol.* 15 (1995) 1938–1944.
- [20] J. Shindo, T. Ishibashi, K. Yokoyama, K. Nakazato, T. Ohwada, M. Shiomi, Y. Maruyama, Granulocyte-macrophage colony-stimulating factor prevents the progression of atherosclerosis via changes in the cellular and extracellular composition of atherosclerotic lesions in Watanabe heritable hyperlipidemic rabbits, *Circulation* 99 (1999) 2150–2156.
- [21] R. Virmani, F.D. Kolodgie, A.P. Burke, A.V. Finn, H.K. Gold, T.N. Tulenko, S.P. Wrenn, J. Narula, Atherosclerotic plaque progression and vulnerability to rupture: angiogenesis as a source of intraplaque hemorrhage, *Arterioscler. Thromb. Vasc. Biol.* 25 (2005) 2054–2061.
- [22] P. Libby, P.M. Ridker, A. Maseri, Inflammation and atherosclerosis, *Circulation* 105 (2002) 1135–1143.
- [23] Y. Sheikine, G.K. Hansson, Chemokines and atherosclerosis, *Ann. Med.* 36 (2004) 98–118.
- [24] G.K. Hansson, Inflammation, atherosclerosis, and coronary artery disease, *N. Engl. J. Med.* 352 (2005) 1685–1695.
- [25] S.O. Heard, M.P. Fink, Counterregulatory control of the acute inflammatory response: granulocyte colony-stimulating factor has anti-inflammatory properties, *Crit. Care Med.* 27 (1999) 1019–1021.
- [26] S. Fujiyama, K. Amano, K. Uehira, M. Yoshida, Y. Nishiwaki, Y. Nozawa, D. Jin, S. Takai, M. Miyazaki, K. Egashira, T. Imada, T. Iwasaka, H. Matsubara, Bone marrow monocyte lineage cells adhere on injured endothelium in a monocyte chemoattractant protein-1-dependent manner and accelerate reendothelialization as endothelial progenitor cells, *Circ. Res.* 93 (2003) 980–989.
- [27] C. Urbich, S. Dimmeler, Endothelial progenitor cells: characterization and role in vascular biology, *Circ. Res.* 95 (2004) 343–353.
- [28] D. Kong, L.G. Melo, M. Gnechi, L. Zhang, G. Mostoslavsky, C.C. Liew, R.E. Pratt, V.J. Dzau, Cytokine-induced mobilization of circulating endothelial progenitor cells enhances repair of injured arteries, *Circulation* 110 (2004) 2039–2046.
- [29] A. Aicher, C. Heeschen, C. Mildner-Rihm, C. Urbich, C. Ihling, K. Technau-Ihling, A.M. Zeiher, S. Dimmeler, Essential role of endothelial nitric oxide synthase for mobilization of stem and progenitor cells, *Nat. Med.* 9 (2003) 1370–1376.
- [30] J. Yu, E.D. deMunck, Z. Zhuang, M. Drinane, K. Kauser, G.M. Rubanyi, H.S. Qian, T. Murata, B. Escalante, W.C. Sessa, Endothelial nitric oxide synthase is critical for ischemic remodeling, mural cell recruitment, and blood flow reserve, *Proc. Natl. Acad. Sci. USA* 102 (2005) 10999–11004.
- [31] E. Jorgensen, R.S. Ripa, S. Helqvist, Y. Wang, H.E. Johnsen, P. Grande, J. Kastrup, In-stent neo-intimal hyperplasia after stem cell mobilization by granulocyte-colony stimulating factor Preliminary intracoronary ultrasound results from a double-blind randomized placebo-controlled study of patients treated with percutaneous coronary intervention for ST-elevation myocardial infarction (STEMMI Trial), *Int. J. Cardiol.* (2005), [Epub ahead of print].
- [32] Y. Wang, K. Tagli, R.S. Ripa, J.C. Nilsson, S. Carstensen, E. Jorgensen, L. Sondergaard, B. Hesse, H.E. Johnsen, J. Kastrup, Effect of mobilization of bone marrow stem cells by granulocyte colony stimulating factor on clinical symptoms, left ventricular perfusion and function in patients with severe chronic ischemic heart disease, *Int. J. Cardiol.* 100 (2005) 477–483.
- [33] F. Kueth, H.R. Figulla, M. Herzau, M. Voth, M. Fritzenwanger, T. Opfermann, K. Pachmann, A. Krack, H.G. Sayer, D. Gottschild, G.S. Werner, Treatment with granulocyte colony-stimulating factor for mobilization of bone marrow cells in patients with acute myocardial infarction, *Am. Heart J.* 150 (2005) 115.
- [34] M. Valgimigli, G.M. Rigolin, C. Citterio, P. Malagutti, S. Curello, G. Percoco, A.M. Bugli, M.D. Porta, L.Z. Bragotti, L. Ansani, E. Mauro, A. Lanfranchi, M. Giganti, L. Feggi, G. Castoldi, R. Ferrari, Use of granulocyte-colony stimulating factor during acute myocardial infarction to enhance bone marrow stem cell mobilization in humans: clinical and angiographic safety profile, *Eur. Heart J.* 26 (2005) 1838–1845.
- [35] H. Ince, M. Petzsch, H.D. Kleine, H. Schmidt, T. Rehders, T. Korber, C. Schumichen, M. Freund, C.A. Nienaber, Preservation from left ventricular remodeling by front-integrated revascularization and stem cell liberation in evolving acute myocardial infarction by use of granulocyte-colony-stimulating factor (FIRSTLINE-AMI), *Circulation* 112 (2005) 3097–3106.

# Critical Roles of Muscle-Secreted Angiogenic Factors in Therapeutic Neovascularization

Kaoru Tateno,\* Tohru Minamino,\* Haruhiro Toko, Hiroshi Akazawa, Naomi Shimizu, Shinichi Takeda, Takeshige Kunieda, Hideyuki Miyauchi, Tomomi Oyama, Katsuhisa Matsuura, Jun-ichiro Nishi, Yoshio Kobayashi, Toshio Nagai, Yoichi Kuwabara, Yoichiro Iwakura, Fumio Nomura, Yasushi Saito, Issei Komuro

**Abstract**—The discovery of bone marrow–derived endothelial progenitors in the peripheral blood has promoted intensive studies on the potential of cell therapy for various human diseases. Accumulating evidence has suggested that implantation of bone marrow mononuclear cells effectively promotes neovascularization in ischemic tissues. It has also been reported that the implanted cells are incorporated not only into the newly formed vessels but also secrete angiogenic factors. However, the mechanism by which cell therapy improves tissue ischemia remains obscure. We enrolled 29 “no-option” patients with critical limb ischemia and treated ischemic limbs by implantation of peripheral mononuclear cells. Cell therapy using peripheral mononuclear cells was very effective for the treatment of limb ischemia, and its efficacy was associated with increases in the plasma levels of angiogenic factors, in particular interleukin-1 $\beta$  (IL-1 $\beta$ ). We then examined an experimental model of limb ischemia using IL-1 $\beta$ –deficient mice. Implantation of IL-1 $\beta$ –deficient mononuclear cells improved tissue ischemia as efficiently as that of wild-type cells. Both wild-type and IL-1 $\beta$ –deficient mononuclear cells increased expression of IL-1 $\beta$  and thus induced angiogenic factors in muscle cells of ischemic limbs to a similar extent. In contrast, inability of muscle cells to secrete IL-1 $\beta$  markedly reduces induction of angiogenic factors and impairs neovascularization by cell implantation. Implanted cells do not secrete angiogenic factors sufficient for neovascularization but, instead, stimulate muscle cells to produce angiogenic factors, thereby promoting neovascularization in ischemic tissues. Further studies will allow us to develop more effective treatments for ischemic vascular disease. (*Circ Res.* 2006;98:1194-1202.)

**Key Words:** angiogenesis ■ interleukins ■ muscles

Peripheral vascular disease (PVD), mainly caused by atherosclerosis, leads to obstruction of the blood supply to the lower or upper extremities. PVD is known to affect 10% to 15% of the adult population in developed countries and is often associated with coronary artery disease.<sup>1</sup> Arteriosclerosis obliterans (ASO) is the most common cause of PVD affecting the lower limbs. Peripheral ischemia can also result from various types of vasculitis, including thromboangiitis obliterans (TAO) or Buerger’s disease, which affects small- and medium-sized arteries and is related to tobacco use and male sex but not to other coronary risk factors. The 2 cardinal symptoms of limb ischemia are intermittent claudication and rest pain: the latter symptom occurs in patients with critical limb ischemia and coincides with ischemic ulceration and gangrene. The treatments of PVD include pharmacotherapy, percutaneous transluminal angioplasty, and vascular surgery and are chosen depending on the

severity of the symptoms and the arteries involved.<sup>2</sup> However, as many as 50% of patients with critical limb ischemia will undergo limb amputation within 1 year because of an insufficient response to the treatments.<sup>1,2</sup>

Recent progress in understanding the mechanisms underlying vascular formation in adults as well as during embryogenesis has opened up a therapeutic avenue for patients without any current options.<sup>3</sup> Initial therapeutic approaches were aimed at delivering angiogenic factors, such as vascular endothelial growth factors (VEGF) and fibroblast growth factor-2, to ischemic tissues by using recombinant proteins or vectors encoding these factors.<sup>4,5</sup> A number of preclinical studies reported improvement of perfusion by such methods in animal models of limb ischemia.<sup>6,7</sup> Although the initial nonrandomized clinical trials showed beneficial effects, the results of controlled clinical trials have not been consistent.<sup>7</sup> More recently, bone marrow–derived circulating endothelial

Original received November 1, 2005; revision received March 9, 2006; accepted March 22, 2006.

From the Departments of Cardiovascular Science and Medicine (K.T., T.M., H.T., H.A., S.T., T.K., H.M., T.O., K.M., J.-i.N., Y. Kobayashi, T.N., Y. Kuwabara, I.K.), Clinical Cell Biology (N.S., Y.S.), and Molecular Diagnosis (F.N.), Chiba University Graduate School of Medicine, Japan; and Division of Cell Biology (Y.I.), Center for Experimental Medicine, Institute of Medical Science, University of Tokyo, Japan.

\*Both authors contributed equally to this study.

Correspondence to Issei Komuro, MD, PhD, Department of Cardiovascular Science and Medicine, Chiba University Graduate School of Medicine, 1-8-1 Inohana, Chuo-ku, Chiba 260-8670, Japan. E-mail komuro-ky@umin.ac.jp

© 2006 American Heart Association, Inc.

*Circulation Research* is available at <http://circres.ahajournals.org>

DOI: 10.1161/01.RES.0000219901.13974.15

progenitors have been identified in the peripheral blood<sup>8,9</sup> and have been shown to contribute to both physiological and pathological angiogenesis in adults.<sup>10,11</sup> These findings have led to the development of therapeutic neovascularization techniques using endothelial progenitors. Preclinical studies indicated that implantation of bone marrow mononuclear cells (BM-MNC), which contain endothelial progenitors, into ischemic limbs was very effective.<sup>12-14</sup> Consequently, this therapeutic strategy was promptly tried for "no-option" patients with critical limb ischemia. The results of the first clinical trial showed that implantation of BM-MNC significantly improved the tissue oxygen concentration and blood flow in ischemic limbs, resulting in a decrease of rest pain and the involution of ischemic ulcers.<sup>15</sup> Although promising results have been obtained, the mechanism by which cell therapy improves limb ischemia is largely unknown. Because direct incorporation of implanted cells into newly formed vessels is reported to be relatively rare, it has been assumed that angiogenic factors secreted by implanted cells are responsible for the efficacy of cell therapy.<sup>16,17</sup>

In the present study, we investigated the efficacy of cell therapy using peripheral blood mononuclear cells (PB-MNC) for the treatment of ischemic limbs. The results of our clinical trial showed that increased levels of angiogenic cytokines correlated with the response to treatment. Implantation of mononuclear cells increased the production of the angiogenic cytokines in muscle cells. A deficiency of the angiogenic cytokines in muscle cells blunted the ability of implanted cells to increase vascularization, suggesting that muscle cells but not mononuclear cells were important as a source of the angiogenic cytokines. Accordingly, we propose a novel mechanism whereby implanted cells promotes neovascularization in ischemic tissues.

## Materials and Methods

### Animals

Generation and genotyping of interleukin (IL)-1 $\beta$ -deficient mice have been previously described.<sup>18</sup> C57BL/6 mice were purchased from SLC Japan. All mice used in this study were 8 to 12 weeks old. All experimental procedures were performed according to the guidelines of Chiba University for animal experiments and the protocols were approved by our institutional review board.

### Collection of Mouse PB-MNC and BM-MNC

Donor mice were euthanized with a lethal dose of anesthetic, after which whole blood or bone marrow were harvested. Mononuclear cells were subsequently separated using Histopaque 1083 (Sigma). To deplete putative endothelial progenitors, the mononuclear cells were further incubated with a rat anti-mouse VEGF receptor-2 antibody (eBiosciences) at a concentration of 0.5  $\mu$ g per 1 million cells. Then the population of cells negative for VEGF receptor-2 was obtained using a magnetic cell sorter (Miltenyi Biotec) according to the instructions of the manufacturer. The control cell population was prepared using an isotype control anti-rat IgG2a antibody. Sorted cells were washed twice with PBS and resuspended in PBS at a concentration of 1 million cells per 100  $\mu$ L for the subsequent experiments. In all experiments, the viability of the mononuclear cells was more than 96.0%, as judged by Trypan blue dye exclusion.

### Hindlimb Ischemia Model

After the mice were anesthetized, the proximal part of the femoral artery and the distal portion of the saphenous artery were ligated and stripped out after all side branches were dissected free. After 24

hours (designated as day 1), either mononuclear cells ( $1.0 \times 10^6$  cells in 100  $\mu$ L of PBS) or PBS (100  $\mu$ L) was injected into the ischemic muscle. As a rescue model, some of the IL-1 $\beta$ -deficient mice were treated with PB-MNC on day 1 and given an intramuscular injection of 0.5 ng of mouse recombinant IL-1 $\beta$  (IBL) on days 3, 5, and 7 after the operation. The mice were euthanized at the indicated times. Before death, hindlimb perfusion was measured with a laser Doppler perfusion analyzer (Moor Instruments).

### Bone Marrow Transplantation Model

Before bone marrow transplantation, 8- to 10-week-old male wild-type or IL-1 $\beta$ -deficient mice were exposed to total body irradiation (9 mGy). Bone marrow cell suspensions were isolated by flushing the femurs and tibias harvested from wild-type or IL-1 $\beta$ -deficient mice. Bone marrow cell suspensions ( $1.5 \times 10^7$  cells) were injected intravenously via the tail vein within 6 hours of irradiation. The chimeric rate was more than 95%, as determined by fluorescence-activated cell sorting analysis of chimeric mice transplanted with bone marrow cells from the green fluorescent protein (GFP) transgenic mice.

### Histology

Vastus and rectus femoris muscle tissues were removed from the ischemic limbs after systemic perfusion with PBS and immediately embedded in OCT compound (Sakura Finetech). Then each specimen was snap frozen in liquid nitrogen and cut into 6- $\mu$ m sections. The sections were stained with antibodies for myosin (MF-20), CD31 (Pharmingen), or IL-1 $\beta$  (Santa Cruz Biotechnology) and counterstained with hematoxylin or 4',6-diamidino-2-phenylindole (DAPI). Two transverse sections of the entire muscle were photographed digitally at a magnification of  $\times 100$  (12 to 16 photographs per mouse), and these photographs were reviewed in a blinded manner. Capillary endothelial cells were identified by immunoreactivity for CD31 and quantified as the number per square millimeter.

### Cell Culture

C2C12 myoblasts were cultured as described previously.<sup>19</sup> Briefly, cells were maintained in DMEM supplemented with 20% FBS (growth medium) until use. In all experiments, the cells were seeded into 60-mm or 100-mm plastic culture dishes at a concentration of  $5 \times 10^3$  cells/cm<sup>2</sup> (day 0) and were incubated at 37°C in a mixture of 95% air and 5% CO<sub>2</sub>. After 24 hours (day 1), the growth medium was changed to DMEM supplemented with 2% horse serum (differentiation medium). On day 4, the medium was replaced by fresh differentiation medium with or without PB-MNC. On day 5, cells were harvested after the mononuclear cells were completely removed by washing 5 times with PBS.

### Statistical Analysis

Data are shown as mean  $\pm$  SEM unless otherwise noted. Changes of the rest pain scale and walking distance over time were analyzed by the rank sum test. Differences of patient background factors between responders and nonresponders were analyzed with the  $\chi^2$  test or Fisher's exact test. Comparison between multiple groups was performed by 1-way ANOVA followed by the Bonferroni procedure for comparison of mean values. Comparisons between two groups were done with the two-tailed Student's *t* test or 2-way ANOVA. For these analyses, of  $P < 0.05$  was considered statistically significant.

An expanded Materials and Methods section is available in the online data supplement at <http://circres.ahajournals.org>.

## Results

### Therapeutic Neovascularization Using PB-MNC for Critical Limb Ischemia

Because most patients with critical limb ischemia have concomitant coronary artery disease and cerebrovascular disease, the collection of bone marrow cells, which requires

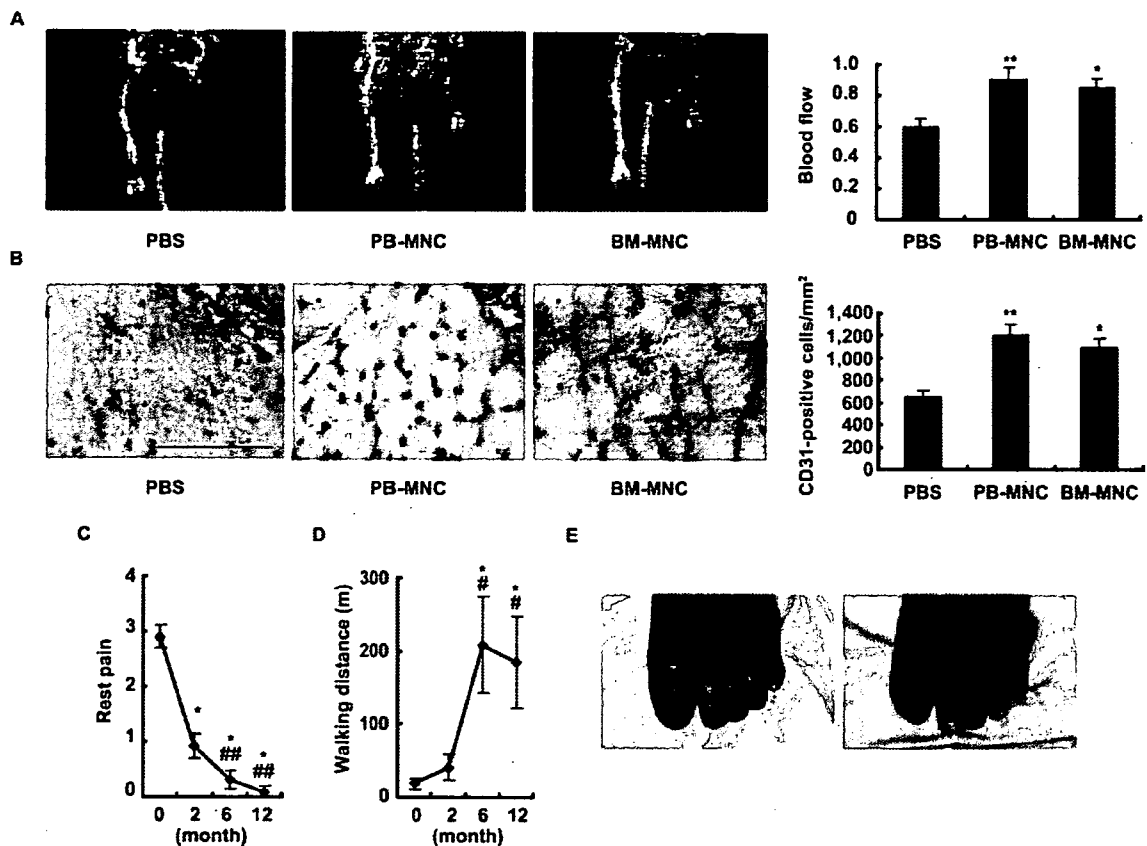


**Figure 1.** Effect of implanting PB-MNC. **A**, Limb perfusion measured by a laser Doppler analyzer at 2 weeks after treatment (photographs). Scale bar=100  $\mu$ m. The graph shows the ratio of ischemic limb (left) to nonischemic limb (right) blood flow. Data are shown as mean $\pm$ SEM. \* $P$ <0.05, \*\* $P$ <0.01 vs PBS-treated group (n=8). **B**, Immunohistochemistry for CD31 (brown) in ischemic limbs at 2 weeks after treatment with PBS, PB-MNC, or BM-MNC. Scale bar=100  $\mu$ m. The number of CD31-positive cells per square millimeter is shown. Data are shown as mean $\pm$ SEM. \* $P$ <0.05, \*\* $P$ <0.01 vs PBS-treated group (n=8). **C**, Changes of the rest pain scale after implantation of PB-MNC. **D**, Improvement of the maximum walking distance after implantation. Data are shown as mean $\pm$ SEM. \* $P$ <0.001 vs 0 month; # $P$ <0.05, ### $P$ <0.001 vs 2 months (n=29). **E**, Nonhealing ischemic ulcer (left) is completely healed by 6 months after implantation (right).

general anesthesia,<sup>15</sup> could cause fatal events in such patients. Given that angiogenic factors secreted from BM-MNC play a major role in cell therapy, PB-MNC may be more beneficial because collection of PB-MNC is much safer and less expensive. To examine the effects implanting PB-MNC, we produced a model of hindlimb ischemia in C57BL/6 mice and implanted PB-MNC into the ischemic limbs of these animals. Implantation of PB-MNC significantly increased perfusion compared with that in the control group (PBS) as assessed by laser Doppler analysis (Figure 1A). The capillary density in ischemic limbs was significantly greater in the PB-MNC group than in the PBS group (Figure 1B). Although BM-MNC has been reported to contain much more ( $\approx$ 100-fold) endothelial progenitors than PB-MNC, there was no significant difference of neovascularization between the PB-MNC group and the BM-MNC group (Figure 1A and 1B), indicating that implantation of PB-MNC is as efficient as BM-MNC for the treatment of limb ischemia and suggesting that endothelial progenitors do not play a pivotal role in the treatment of limb ischemia at least by PB-MNC.

After obtaining approval from the ethical committee of Chiba University Graduate School of Medicine, we started a

pilot clinical trial to investigate whether therapeutic neovascularization by implantation of PB-MNC is feasible and effective for ischemic limbs. We enrolled 29 patients with critical limb ischemia caused by ASO or TAO who had no treatment options. More than 80% of the patients were recommended to undergo major amputation by their doctors before enrollment because of unhealed ischemic ulcers or gangrene despite conventional therapy (Tables 1 and 2). Approximately half of the patients had chronic renal failure and were on dialysis 3 times weekly (Table 1). Apart from 5 TAO subjects, most of the patients (82.7%) had 1 or more complications (Table 1). We implanted PB-MNC into the ischemic limbs of these patients twice within a 1-month period and estimated their response at 2 months, 6 months, and 1 year after treatment (as described in the online data supplement). Rest pain was significantly decreased and was nearly normalized by 1 year after treatment (Figure 1C). The maximum walking distance also improved significantly, and this improvement was preserved for a year (Figure 1D). Three patients (11.1%) underwent major amputation, which was much less frequent compared with the reported annual rate of amputation in patients with critical limb ischemia ( $\approx$ 50%).<sup>2</sup>



**TABLE 1. Patient Background**

Age, y	61.8±11.3
Gender	
Male	24 (82.8%)
Female	5 (17.2%)
Diagnosis	
ASO	19 (65.5%)
TAO	10 (34.5%)
Ischemic status	
Fontaine 3	4 (13.8%)
Fontaine 4	25 (86.2%)
Previous treatment	
PTA	7 (24.1%)
Bypass surgery	2 (6.9%)
ABPI	0.79±0.26
Rest pain scale	2.90±1.11
Complications	
CRF on HD	14 (48.3%)
CAD	13 (44.8%)
CVD	8 (27.6%)
Diabetes	16 (55.2%)
Hyperlipidemia	16 (55.2%)
Hypertension	13 (44.8%)
Any complications	24 (82.7%)

Data are shown as mean±SD or the no. of patients (%). PTA indicates percutaneous transluminal angioplasty; CRF, chronic renal failure; HD, hemodialysis; CAD, coronary artery disease; CVD, cerebrovascular disease.

Improvement of ischemic ulcers was observed 16 of 24 patients (66.7%) (Figure 1E), whereas only 31% of the patients showed substantial improvement of the ankle-brachial pressure index (ABPI), presumably because of underestimation of improvement in this index of hemodialysis patients. There were no major complications related to the treatment, such as death or coronary events. Three patients died of unrelated causes, including pneumonia and chronic renal failure (11.1%), which was lower than the reported annual mortality rate of patients with critical limb ischemia (~25%).<sup>1</sup> These results indicate that implantation of PB-MNC was a safe and effective treatment for critical limb ischemia.

**Factors Associated With the Response to Treatment**

We next investigated the factors related to the response to treatment. We divided the patients into a group of responders (n=21) and a group of nonresponders (n=8) according to a response score estimated from the improvement of rest pain, ischemic ulcers, walking distance, and ABPI. Then we compared their background factors and laboratory data. There were no significant differences of patient background factors, including age, gender, and coronary risk factors, between responders and nonresponders (Table 2). The serum level of C-reactive protein, a marker of inflammation induced by cytokines, was significantly higher in the responders after implantation (Table 2). Therefore, we examined the plasma

**TABLE 2. Clinical Response and Patient Background**

	Nonresponders (n=8)	Responders (n=21)	P
Age, y	60.6±11.7	62.3±11.3	NS
Gender			
Male	7 (87.5%)	17 (81.0%)	NS
Female	1 (12.5%)	4 (19.0%)	
Diagnosis			
ASO	6 (75.0%)	13 (61.9%)	NS
TAO	2 (25.0%)	8 (38.1%)	
Ischemic status			
Fontaine 3	1 (12.5%)	3 (14.3%)	NS
Fontaine 4	7 (87.5%)	18 (85.7%)	NS
Previous revascularization	3 (37.5%)	5 (23.8%)	NS
Duration of illness (month)	19.6±24.0	52.1±55.8	NS
ABPI	0.85±0.20	0.77±0.28	NS
Rest pain scale	2.90±1.40	2.90±1.00	NS
Need for major amputation	8 (80.0%)	13 (61.9%)	NS
Complications			
CRF on HD	4 (50.0%)	10 (47.6%)	NS
CAD	4 (50.0%)	9 (42.9%)	NS
LVEF (%)	48.1±28.4	48.2±28.1	NS
CVD	3 (37.5%)	5 (23.8%)	NS
Diabetes	6 (75.0%)	10 (47.6%)	NS
Hyperlipidemia	4 (50.0%)	12 (57.1%)	NS
Hypertension	4 (50.0%)	9 (42.9%)	NS
MBP (mm Hg)	81.0±34.1	86.8±31.9	NS
Laboratory data			
FBS (mg/dL)	139.6±45.1	133.2±49.3	NS
HbA <sub>1c</sub> (%)	5.6±0.9	5.8±0.9	NS
T-Cho (mg/dL)	169.8±33.2	184.6±37.2	NS
LDL-Cho (mg/dL)	105.6±24.6	114.8±32.7	NS
HDL-Cho (mg/dL)	43.9±10.0	49.7±10.7	NS
CRP (mg/dL)	2.9±3.8	5.4±11.0	0.018

Data are shown as mean±SD or the no. of patients (%). CRF indicates chronic renal failure; HD, hemodialysis; CAD, coronary artery disease; LVEF, left ventricular ejection fraction; CVD, cerebrovascular disease; MBP, mean blood pressure; FBS, fasting blood sugar; T-Cho, total cholesterol; Cho, cholesterol; CRP, C-reactive protein. Patients with osteomyelitis were excluded for analysis of CRP data.

levels of various angiogenic cytokines in the patients at days 1, 3, 7, and 14 after implantation. We found that the peak levels of IL-1β, IL-6, and VEGF, but not tumor necrosis factor-α or granulocyte colony-stimulating factor, were markedly higher in responders than in nonresponders (Figure 2A; Figure I in the online data supplement). In contrast, there were no significant differences of the number of implanted mononuclear cells and CD34-positive cells between the 2 groups (Figure 2A). Consistent with these results, deprivation of putative endothelial progenitors (VEGF receptor-2-positive cells) did not affect the ability of implanted mononuclear cells to promote neovascularization in a mouse model of hindlimb ischemia (Figure 2B). Thus, we speculated that the

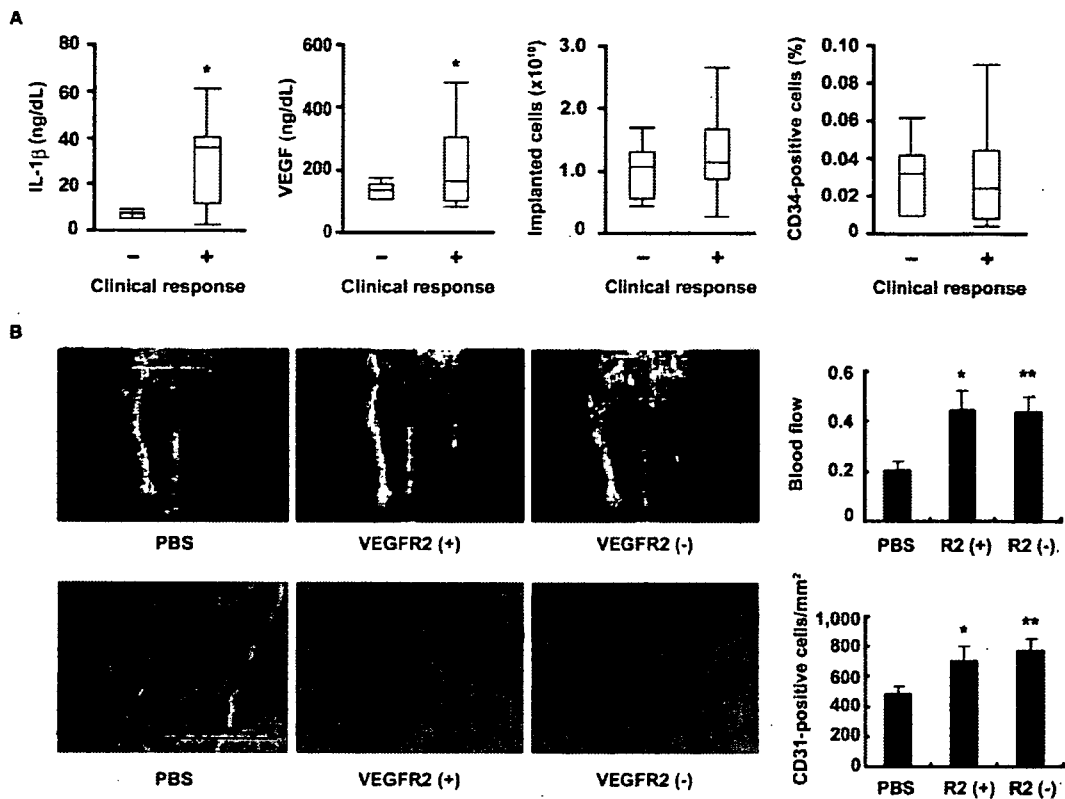


**Figure 2.** Factors associated with the response to treatment. A, Results are shown as box plots representing median, 25th and 75th percentiles as boxes and the range of data as bars. \* $P < 0.05$  vs nonresponders (responders,  $n = 21$ ; nonresponders,  $n = 8$ ). B, Depletion of VEGF receptor 2 (VEGFR2)-positive mononuclear cells did not affect the ability of implanted cells to promote increases of perfusion (upper) and capillary density (lower) at 1 week after implantation. Scale bar = 100  $\mu\text{m}$ . R2(-): VEGFR2-depleted mononuclear cells. R2(+): control mononuclear cells. Data are shown as mean  $\pm$  SEM. \* $P < 0.05$ , \*\* $P < 0.01$  vs PBS-treated group ( $n = 8$ ).

increase of angiogenic factors secreted by implanted mononuclear cells might influence the efficacy of this therapy.

### Increased Expression of IL-1 $\beta$ in Ischemic Limbs Is Crucial for Neovascularization

Because IL-1 $\beta$  is known to be a potent angiogenic cytokine and induces a number of angiogenic factors including VEGF,<sup>20,21</sup> we examined the role of IL-1 $\beta$  on neovascularization induced by mononuclear cell implantation in a model of hindlimb ischemia. When PB-MNC from wild-type mice were implanted into the ischemic limbs of wild-type mice, blood flow and capillary density were significantly increased compared with those in a PBS-treated group (Figure 3A and 3B). Unexpectedly, PB-MNC derived from IL-1 $\beta$ -deficient mice<sup>18</sup> increased the blood flow of the ischemic limbs in wild-type mice as efficiently as wild-type PB-MNC (Figure 3A). Likewise, implantation of IL-1 $\beta$ -deficient PB-MNC significantly increased capillary density compared with the PBS-treated group (Figure 3B). In contrast, implantation of wild-type PB-MNC into ischemic limbs of IL-1 $\beta$ -deficient mice had no effect on neovascularization (Figure 3A and 3B), suggesting that increased expression of IL-1 $\beta$  in ischemic limbs is more important for neovascularization than expression by implanted cells. Expression of VEGF in the ischemic limbs of wild-type mice was significantly elevated by implantation of IL-1 $\beta$ -deficient PB-MNC as well as wild-type PB-MNC compared with the PBS-treated group (Figure 3C).

However, implantation of wild-type PB-MNC failed to induce VEGF expression in the ischemic limbs of IL-1 $\beta$ -deficient mice (Figure 3C). The pattern of IL-1 $\beta$  expression in ischemic limbs was very similar to that of VEGF (Figure 3D). A significant increase of IL-1 $\beta$  expression was observed in the ischemic limbs of wild-type mice treated with wild-type or IL-1 $\beta$ -deficient PB-MNC, whereas there was no induction of IL-1 $\beta$  in the ischemic limbs of IL-1 $\beta$ -deficient mice after implantation of wild-type PB-MNC (Figure 3D). These results suggest that implantation of PB-MNC induces IL-1 $\beta$  expression in ischemic limbs and promotes neovascularization by the induction of angiogenic factors such as VEGF.

Previous studies demonstrated that infiltration of macrophages plays a critical role in IL-1 $\beta$ -induced neovascularization.<sup>22,23</sup> To test this, we injected PB-MNC from GFP transgenic mice into the ischemic limbs of wild-type or IL-1 $\beta$ -deficient mice and performed histological analyses at 5 days after treatment. The number of infiltrating host-derived (GFP-negative) macrophages was significantly fewer in the ischemic limbs of IL-1 $\beta$ -deficient mice than in those of wild-type mice (supplemental Figure II). PB-MNC implantation significantly induced macrophage infiltration compared with PBS-treated mice (supplemental Figure II). There was no difference in infiltration of macrophages into nonischemic limbs between wild-type and IL-1 $\beta$ -deficient mice

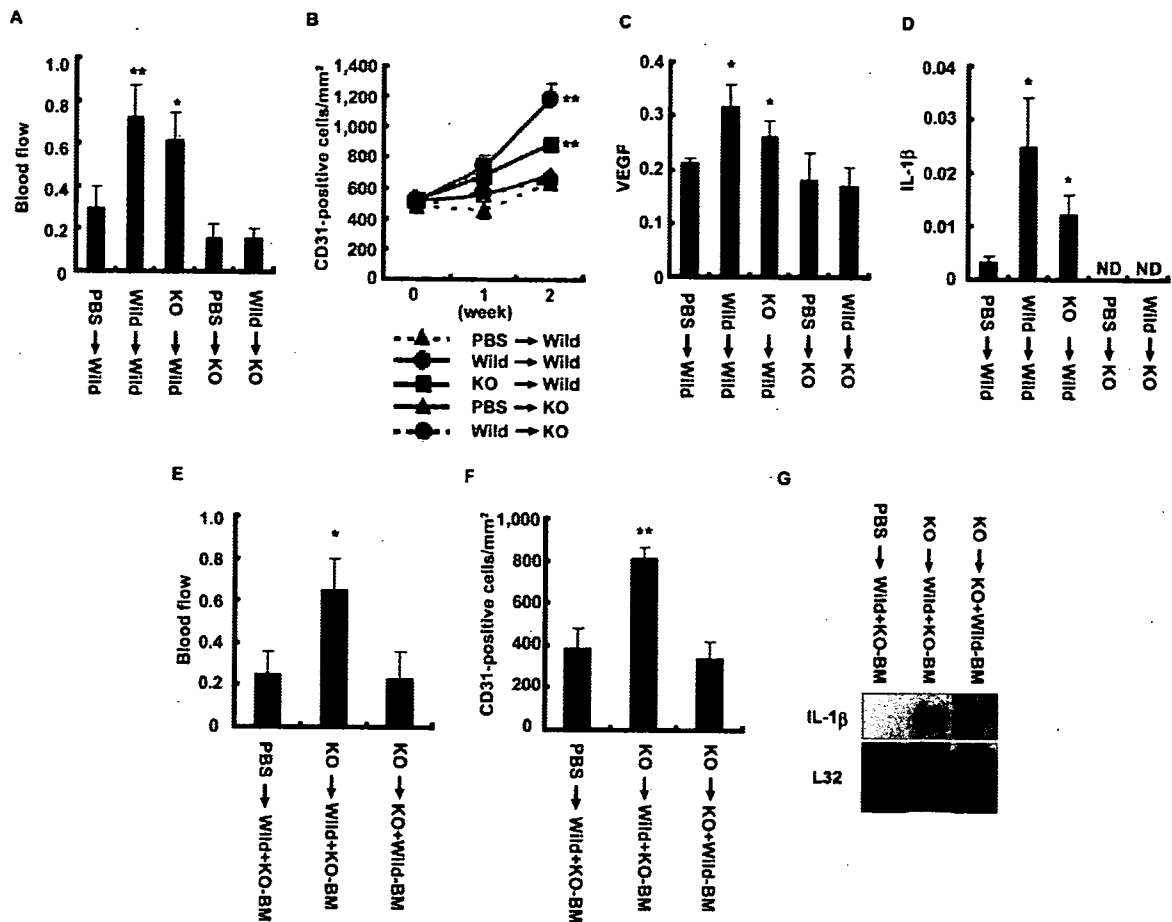


**Figure 3.** Impairment of PB-MNC-induced neovascularization in IL-1 $\beta$ -deficient mice. **A**, The graph shows relative blood flow in the ischemic limbs of wild-type mice treated with PBS (PBS→Wild), wild-type PB-MNC (Wild→Wild), or IL-1 $\beta$ -deficient PB-MNC (KO→Wild) and the limbs of IL-1 $\beta$ -deficient mice treated with PBS (PBS→KO) or wild-type PB-MNC (Wild→KO). **B**, Immunohistochemistry for CD31 in ischemic limbs. **C**, Expression of VEGF in ischemic limbs of the same mice at 1 week after treatment was analyzed by the ribonuclease protection assay (RPA). Relative expression to that of L32 (the internal control) is shown. **D**, Expression of IL-1 $\beta$  in ischemic limbs of the same mice at 1 week after implantation was analyzed by RPA and relative expression to that of L32 is shown. ND indicates not detected. Data are shown as mean $\pm$ SEM. \* $P$ <0.05, \*\* $P$ <0.01 vs wild-type mice treated with PBS ( $n$ =5). **E**, **F**, and **G**, The graph shows blood flow (**E**), capillary density (**F**), and expression of IL-1 $\beta$  (**G**) in the ischemic limbs of wild-type mice with IL-1 $\beta$ -deficient bone marrow treated with PBS (PBS→Wild+KO-BM) or IL-1 $\beta$ -deficient PB-MNC (KO→Wild+KO-BM) and the limbs of IL-1 $\beta$ -deficient mice with wild-type bone marrow treated with IL-1 $\beta$ -deficient PB-MNC (KO→KO+Wild-BM). The values are shown as described in the legend of Figure 1A for blood flow and capillary density. Data are shown as mean $\pm$ SEM. \* $P$ <0.05, \*\* $P$ <0.01 vs PBS→Wild+KO-BM ( $n$ =5).

(supplemental Figure II). Thus, infiltration of macrophages may be also involved in the mechanisms underlying IL-1 $\beta$ -induced neovascularization.

To investigate whether host-derived hematopoietic cells contribute to induction of IL-1 $\beta$  by mononuclear cell implantation, we produced chimeric mice. When PB-MNC from IL-1 $\beta$ -deficient mice were implanted into the ischemic limbs of wild-type mice with IL-1 $\beta$ -deficient bone marrow, blood flow and capillary density were significantly increased compared with those in a PBS-treated group (Figure 3E and 3F). In contrast, injection of IL-1 $\beta$ -deficient PB-MNC into the ischemic limbs of IL-1 $\beta$ -deficient mice with wild-type bone marrow did not enhance neovascularization (Figure 3A, 3B, 3E, and 3F). Consistent with these results, PB-MNC implantation markedly induced IL-1 $\beta$  expression in the ischemic limbs of wild-type mice with IL-1 $\beta$ -deficient bone marrow compared with the limbs of IL-1 $\beta$ -deficient mice with

wild-type bone marrow (Figure 3G), which suggests a minor role of host-derived hematopoietic cells in the production of IL-1 $\beta$  after treatment.

### Critical Roles of Muscle-Secreted Angiogenic Factors

To determine the type of cells in which IL-1 $\beta$  expression is induced by implantation of PB-MNC, we performed immunohistochemical analysis of ischemic limbs after implantation. Expression of IL-1 $\beta$  was localized to the skeletal muscle cells, as identified by staining for sarcomeric myosin, and was particularly detected in the regenerating tissues (Figure 4A). Likewise, in situ hybridization revealed that IL-1 $\beta$  was predominantly expressed by muscle cells and, to a lesser extent, by other types of cells such as vascular cells and infiltrating leukocytes (Figure 4B and data not shown). To test whether PB-MNC could increase the expression of

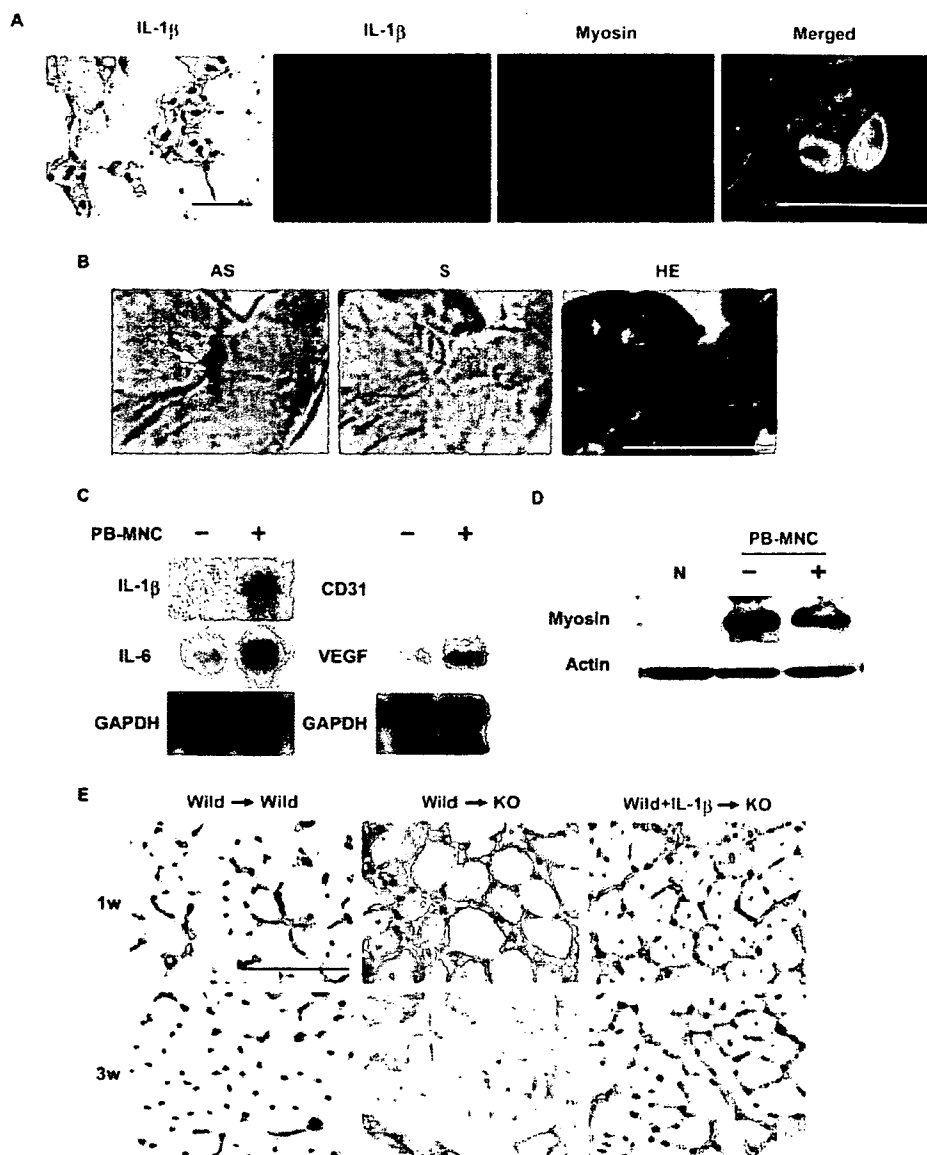


**Figure 4.** Mononuclear cell implantation increases the production of angiogenic factors by muscle cells. **A**, Left photograph shows immunohistochemistry for IL-1 $\beta$  (brown) in ischemic limbs at 5 days after implantation. Right photographs indicate immunofluorescence for IL-1 $\beta$  (red), myosin (green), and the nuclei (blue). Scale bar=50  $\mu$ m. **B**, In situ hybridization for IL-1 $\beta$  (arrow) in ischemic limbs at 5 days after implantation. AS indicates anti-sense probe; S, sense probe; HE, hematoxylin/eosin staining. **C**, C2C12 cells were cultured under differentiating conditions with or without PB-MNC ( $2.5 \times 10^5$  cells/mL) for 24 hours, and expression of angiogenic cytokines was examined by RPA. Glyceraldehyde-3-phosphate dehydrogenase (GAPDH) was used as the control. **D**, C2C12 cells with or without PB-MNC were examined for myosin expression by Western blot analysis. Actin was used as the loading control. Undifferentiated C2C12 cells were used as a negative control (N). **E**, Immunohistochemistry for CD31 in the ischemic limbs of wild-type mice treated with wild-type PB-MNC (Wild $\rightarrow$ Wild) and the limbs of IL-1 $\beta$ -deficient mice treated with wild-type PB-MNC (Wild $\rightarrow$ KO), or wild-type PB-MNC plus IL-1 $\beta$  (Wild+IL-1 $\beta$  $\rightarrow$ KO) at 1 week (left) and 3 weeks (right) after implantation. Scale bar=100  $\mu$ m.

angiogenic cytokines by muscle cells, we cocultured mouse embryonic muscle cells (C2C12) with PB-MNC from wild-type mice for 24 hours under differentiating conditions and harvested muscle cells after intensive wash with PBS to eliminate PB-MNC from the samples. Cocultivation with PB-MNC increased the expression of various angiogenic cytokines such as IL-1 $\beta$ , IL-6, and VEGF by C2C12 cells (Figure 4C). C2C12 cells treated with PB-MNC as well as nontreated cells expressed myosin (Figure 4D), whereas expression of CD31 was not detected in these cells (Figure 4C), indicating that contamination of PB-MNC was negligible. Cocultivation of C2C12 cells with human PB-MNC also induced expression of mouse cytokines as determined by RPA using a mouse-specific probe (supplemental Figure III). We, therefore, concluded that implantation of mononuclear cells promotes neovascularization by stimulating muscle cells to increase the production of angiogenic cytokines such as IL-1 $\beta$ .

We then examined whether treatment with IL-1 $\beta$  restores the efficacy of PB-MNC implantation in the ischemic limbs of IL-1 $\beta$ -deficient mice. We observed that neovascularization occurred in the ischemic tissues at 1 week and that the appearance of the skeletal muscles became normal by 3 weeks after implantation (Figure 4E). Implantation of wild-type PB-MNC did not induce neovascularization in the ischemic limbs of IL-1 $\beta$ -deficient mice at 1 week, and, thus, necrosis occurred by 3 weeks after implantation (Figure 4E). In contrast, administration of IL-1 $\beta$  in conjunction with implantation of wild-type PB-MNC significantly increased neovascularization ( $P < 0.01$  versus IL-1 $\beta$ -deficient mice treated with wild-type PB-MNC;  $n = 3$ ) and prevented necrosis of the ischemic limbs in IL-1 $\beta$ -deficient mice at 3 weeks (Figure 4E). Consistent with the results of histological analyses, improvement of blood flow by PB-MNC implantation in wild-type mice was significantly better than in IL-1 $\beta$ -deficient mice (Figure 3A and supplemental Figure IV).

Moreover, administration of IL-1 $\beta$  in conjunction with implantation of wild-type PB-MNC partially improved the effect of PB-MNC implantation on blood flow in IL-1 $\beta$ -deficient mice (supplemental Figure IV). However, administration of IL-1 $\beta$  without PB-MNC implantation did not improve limb ischemia in wild-type mice (supplemental Figure V). Thus, it is conceivable that induction of IL-1 $\beta$  is prerequisite for the efficacy of PB-MNC implantation, but an IL-1 $\beta$  only treatment is insufficient for limb salvage.

### Discussion

The present study provided a possible mechanism for the process of neovascularization during cell therapy for limb ischemia. The results of our clinical trial showed that angiogenic cytokines, especially IL-1 $\beta$ , were associated with the response to treatment. Many previous studies have suggested that angiogenic factors secreted by implanted cells play a critical role in therapeutic neovascularization.<sup>16,17</sup> In contrast, our *in vitro* and *in vivo* studies demonstrated that the implanted mononuclear cells did not secrete cytokines sufficient for neovascularization but, instead, stimulated muscle cells to produce IL-1 $\beta$ . This is consistent with our observation that most of the implanted cells disappeared from the ischemic tissues as early as 3 days after implantation, which was before reconstruction of the vascular system started (K.T., T.M., I.K., unpublished data, 2006). Thus, it is likely that muscle cells but not implanted cells are a major source of angiogenic cytokines in ischemic limbs.

We noted that IL-1 $\beta$  was predominantly expressed by myocytes with central nuclei in ischemic limbs, indicating that these cells are regenerating myocytes (Figure 4A). We also observed that implantation of mononuclear cells increased the number of central nucleated myocytes in ischemic limbs (K.T., T.M., I.K., unpublished data, 2006). We therefore propose a novel model of neovascularization, in which implanted mononuclear cells enhance muscle regeneration and the increased expression of IL-1 $\beta$  by regenerating myocytes promotes neovascularization via induction of angiogenic factors, thereby contributing to limb salvage. Implantation of wild-type mononuclear cells increased the number of regenerating myocytes in the ischemic limbs of IL-1 $\beta$ -deficient mice compared with PBS-treated IL-1 $\beta$ -deficient mice (Figure 4E and supplemental Figure VI). However, the regeneration of myocytes was not accompanied by neovascularization at 1 week, and, thus, necrosis occurred by 3 weeks after implantation (Figure 4E). These results suggest that implantation of mononuclear cells promotes muscle regeneration and that the regenerated muscle-secreted IL-1 $\beta$  induces neovascularization, leading to suitable conditions for further muscle regeneration. Thus, although expression of IL-1 $\beta$  by muscle cells is required for mononuclear cells promoting neovascularization, administration of IL-1 $\beta$  could not obviate the need for injection of mononuclear cells.

We recently reported a similar finding that granulocyte colony-stimulating factor acts directly on cardiomyocytes and promotes neovascularization in ischemic myocardium by inducing the production of angiogenic factors.<sup>24</sup> Our results also coincide with recent evidence suggesting an important role for the interaction between macrophages and skeletal

muscle in the process of muscle regeneration after injury.<sup>25</sup> During this process, muscle cells modulate macrophage invasion by releasing cytokines such as monocyte chemoattractant protein-1 and VEGF.<sup>26</sup> On the other hand, macrophages release factors *in vitro* that promote the proliferation of muscle cells.<sup>27</sup> Macrophages are also present *in vivo* at sites where muscle regeneration occurs,<sup>28</sup> and macrophage depletion significantly impairs muscle regeneration after transplantation of myogenic cells,<sup>29</sup> suggesting a critical role of macrophages in muscle repair. However, there are no definitive studies to show which factors (if any) are released by macrophages *in vivo* to influence the process of muscle repair. In our study, it is unclear how the implanted mononuclear cells stimulated muscle cells to proliferate and induce the expression of angiogenic factors. It would be also interesting to determine whether the similar mechanisms are involved in other modes of therapeutic vascularization such as cytokine therapy. Further studies on the roles of cellular communications will allow us to develop more effective treatments for ischemic vascular disease.

### Acknowledgments

This work was supported by a grant-in-aid for scientific research and developmental scientific research from the Ministry of Education, Science, Sports, and Culture, Health and Labor Sciences Research Grants (to I.K.) and grants from the Japan Research Foundation for Clinical Pharmacology, NOVARTIS foundation, and the Ministry of Education, Science, Sports, and Culture of Japan (to T.M.).

### References

- Braunwald E, Zipes DP, Libby P. *Heart Disease: A Textbook of Cardiovascular Medicine*. 6th ed. Philadelphia: Saunders; 2001.
- Dormandy JA, Rutherford RB. Management of peripheral arterial disease (PAD). TASC Working Group. TransAtlantic Inter-Society Consensus (TASC). *J Vasc Surg*. 2000;31:S1-S296.
- Carmeliet P. Mechanisms of angiogenesis and arteriogenesis. *Nat Med*. 2000;6:389-395.
- Takeshita S, Zheng LP, Brogi E, Kearney M, Pu LQ, Bunting S, Ferrara N, Symes JF, Isner JM. Therapeutic angiogenesis. A single intraarterial bolus of vascular endothelial growth factor augments revascularization in a rabbit ischemic hind limb model. *J Clin Invest*. 1994;93:662-670.
- Harada K, Grossman W, Friedman M, Edelman ER, Prasad PV, Keighley CS, Manning WJ, Sellke FW, Simons M. Basic fibroblast growth factor improves myocardial function in chronically ischemic porcine hearts. *J Clin Invest*. 1994;94:623-630.
- Ferrara N, Alitalo K. Clinical applications of angiogenic growth factors and their inhibitors. *Nat Med*. 1999;5:1359-1364.
- Yla-Herttuala S, Alitalo K. Gene transfer as a tool to induce therapeutic vascular growth. *Nat Med*. 2003;9:694-701.
- Asahara T, Murohara T, Sullivan A, Silver M, van der Zee R, Li T, Witzenbichler B, Schatteman G, Isner JM. Isolation of putative progenitor endothelial cells for angiogenesis. *Science*. 1997;275:964-967.
- Shi Q, Rafii S, Wu MH, Wijelath ES, Yu C, Ishida A, Fujita Y, Kothari S, Mohle R, Sauvage LR, Moore MA, Storb RF, Hammond WP. Evidence for circulating bone marrow-derived endothelial cells. *Blood*. 1998;92:362-367.
- Asahara T, Masuda H, Takahashi T, Kalka C, Pastore C, Silver M, Kearney M, Magner M, Isner JM. Bone marrow origin of endothelial progenitor cells responsible for postnatal vasculogenesis in physiological and pathological neovascularization. *Circ Res*. 1999;85:221-228.
- Rafii S, Lyden D. Therapeutic stem and progenitor cell transplantation for organ vascularization and regeneration. *Nat Med*. 2003;9:702-712.
- Ikenaga S, Hamano K, Nishida M, Kobayashi T, Li TS, Kobayashi S, Matsuzaki M, Zempo N, Esato K. Autologous bone marrow implantation induced angiogenesis and improved deteriorated exercise capacity in a rat ischemic hindlimb model. *J Surg Res*. 2001;96:277-283.

13. Shintani S, Murohara T, Ikeda H, Ueno T, Sasaki K, Duan J, Imaizumi T. Augmentation of postnatal neovascularization with autologous bone marrow transplantation. *Circulation*. 2001;103:897-903.
14. Li TS, Hamano K, Suzuki K, Ito H, Zempo N, Matsuzaki M. Improved angiogenic potency by implantation of ex vivo hypoxia prestimulated bone marrow cells in rats. *Am J Physiol Heart Circ Physiol*. 2002;283:H468-H473.
15. Tateishi-Yuyama E, Matsubara H, Murohara T, Ikeda U, Shintani S, Masaki H, Amano K, Kishimoto Y, Yoshimoto K, Akashi H, Shimada K, Iwasaka T, Imaizumi T. Therapeutic angiogenesis for patients with limb ischaemia by autologous transplantation of bone-marrow cells: a pilot study and a randomised controlled trial. *Lancet*. 2002;360:427-435.
16. Urbich C, Dimmeler S. Endothelial progenitor cells: characterization and role in vascular biology. *Circ Res*. 2004;95:343-353.
17. Kinnaird T, Stabile E, Burnett MS, Epstein SE. Bone-marrow-derived cells for enhancing collateral development: mechanisms, animal data, and initial clinical experiences. *Circ Res*. 2004;95:354-363.
18. Horai R, Asano M, Sudo K, Kanuka H, Suzuki M, Nishihara M, Takahashi M, Iwakura Y. Production of mice deficient in genes for interleukin (IL)-1alpha, IL-1beta, IL-1alpha/beta, and IL-1 receptor antagonist shows that IL-1beta is crucial in turpentine-induced fever development and glucocorticoid secretion. *J Exp Med*. 1998;187:1463-1475.
19. Takahashi A, Kureishi Y, Yang J, Luo Z, Guo K, Mukhopadhyay D, Ivashchenko Y, Branellec D, Walsh K. Myogenic Akt signaling regulates blood vessel recruitment during myofiber growth. *Mol Cell Biol*. 2002;22:4803-4814.
20. Voronov E, Shouval DS, Krelm Y, Cagnano E, Benharroch D, Iwakura Y, Dinarello CA, Apte RN. IL-1 is required for tumor invasiveness and angiogenesis. *Proc Natl Acad Sci U S A*. 2003;100:2645-2650.
21. El Awad B, Kreft B, Wolber EM, Hellwig-Burgel T, Metzén E, Fandrey J, Jelkmann W. Hypoxia and interleukin-1beta stimulate vascular endothelial growth factor production in human proximal tubular cells. *Kidney Int*. 2000;58:43-50.
22. Nakao S, Kuwano T, Tsutsumi-Miyahara C, Ueda S, Kimura YN, Hamano S, Sonoda KH, Saijo Y, Nukiwa T, Strieter RM, Ishibashi T, Kuwano M, Ono M. Infiltration of COX-2-expressing macrophages is a prerequisite for IL-1beta-induced neovascularization and tumor growth. *J Clin Invest*. 2005;115:2979-2991.
23. Saijo Y, Tanaka M, Miki M, Usui K, Suzuki T, Maemondo M, Hong X, Tazawa R, Kikuchi T, Matsushima K, Nukiwa T. Proinflammatory cytokine IL-1 beta promotes tumor growth of Lewis lung carcinoma by induction of angiogenic factors: in vivo analysis of tumor-stromal interaction. *J Immunol*. 2002;169:469-475.
24. Harada M, Qin Y, Takano H, Minamino T, Zou Y, Toko H, Ohtsuka M, Matsuura K, Sano M, Nishi J, Iwanaga K, Akazawa H, Kunieda T, Zhu W, Hasegawa H, Kunisada K, Nagai T, Nakaya H, Yamauchi-Takahara K, Komuro I. G-CSF prevents cardiac remodeling after myocardial infarction by activating the Jak-Stat pathway in cardiomyocytes. *Nat Med*. 2005;11:305-311.
25. Tidball JG. Inflammatory processes in muscle injury and repair. *Am J Physiol Regul Integr Comp Physiol*. 2005;288:R345-R353.
26. Chazaud B, Sonnet C, Lafuste P, Bassez G, Rimaniol AC, Poron F, Authier FJ, Dreyfus PA, Gherardi RK. Satellite cells attract monocytes and use macrophages as a support to escape apoptosis and enhance muscle growth. *J Cell Biol*. 2003;163:1133-1143.
27. Massimino ML, Rapizzi E, Cantini M, Libera LD, Mazzoleni F, Arslan P, Carraro U. ED2+ macrophages increase selectively myoblast proliferation in muscle cultures. *Biochem Biophys Res Commun*. 1997;235:754-759.
28. Pimorady-Esfahani A, Grounds MD, McMenamin PG. Macrophages and dendritic cells in normal and regenerating murine skeletal muscle. *Muscle Nerve*. 1997;20:158-166.
29. Lescaudron L, Peltekian E, Fontaine-Perus J, Paulin D, Zampieri M, Garcia L, Parrish E. Blood borne macrophages are essential for the triggering of muscle regeneration following muscle transplant. *Neuro-muscul Disord*. 1999;9:72-80.

### Granulocyte Colony Stimulating Factor Directly Inhibits Myocardial Ischemia-Reperfusion Injury Through Akt-Endothelial NO Synthase Pathway

Kazutaka Ueda, Hiroyuki Takano, Hiroshi Hasegawa, Yuriko Niitsuma, Yingjie Qin, Masashi Ohtsuka, Issei Komuro

**Objective**—Granulocyte colony stimulating factor (G-CSF) has been reported recently to prevent cardiac remodeling and dysfunction after acute myocardial infarction through signal transducer and activator of transcription 3 (STAT3). In this study, we examined acute effects of G-CSF on the heart against ischemia-reperfusion injury.

**Methods and Results**—Rat hearts were subjected to global 35-minute ischemia and 120-minute reperfusion in Langendorff system with or without G-CSF (300 ng/mL). G-CSF administration was started at the onset of reperfusion. Triphenyltetrazolium chloride staining revealed that G-CSF markedly reduced the infarct size. G-CSF strongly activated Janus kinase 2 (Jak2), STAT3, extracellular signal-regulated kinase (ERK), Akt, and endothelial NO synthase (NOS) in the hearts subjected to ischemia followed by 15-minute reperfusion. The G-CSF-induced reduction in infarct size was abolished by inhibitors of phosphatidylinositol 3-kinase, Jak2, and NOS but not of mitogen-activated protein kinase kinase (MEK).

**Conclusions**—These results suggest that G-CSF acts directly on the myocardium during ischemia-reperfusion injury and has acute nongenomic cardioprotective effects through the Akt-endothelial NOS pathway. (*Arterioscler Thromb Vasc Biol.* 2006;26:e108-e113.)

**Key Words:** G-CSF ■ reperfusion injury ■ cytokine ■ nitric oxide synthase ■ signal transduction

Myocardial infarction (MI) is the most common cause of cardiac morbidity and mortality in many countries. Reperfusion therapy is beneficial to prevent cardiomyocyte death and contractile dysfunction after MI. However, numerous studies have shown that reperfusion itself may enhance the injury, resulting in extension of infarct size after ischemia (ie, ischemia-reperfusion [IR] injury). Although ischemic preconditioning and pharmacological preconditioning mimetics strongly protect the heart against IR injury, the requirement for pretreatment has greatly limited their clinical relevance. Meanwhile, it has been reported recently that brief intermittent ischemia applied after the onset of reperfusion, termed "postconditioning," reduces myocardial injury to an extent comparable to preconditioning.<sup>1</sup> Various cardioprotective mechanisms have been reported including activation of reperfusion injury salvage kinases pathway consisting of phosphatidylinositol 3-kinase (PI3K)-Akt and extracellular signal-regulated kinase (ERK).<sup>2</sup> Therefore, pharmacological

postconditioning by administration of agents that activate the reperfusion injury salvage kinase pathway seems to be beneficial to IR injury.

Granulocyte colony stimulating factor (G-CSF) has been reported recently to prevent left ventricular (LV) remodeling and dysfunction after acute MI.<sup>3-6</sup> G-CSF is a hematopoietic cytokine that promotes proliferation and differentiation of neutrophil progenitors. Because G-CSF has been used widely to induce mobilization of hematopoietic stem cells for transplantation, and the safety has been established, G-CSF could be used to treat MI if the efficacy has been established and the mechanisms of its beneficial effects have been elucidated. We demonstrated that G-CSF phosphorylates and activates various signaling pathways such as Akt, ERK, and Janus kinase 2 (Jak2)-signal transducer and activator of transcription 3 (STAT3) through G-CSF receptors on cardiac myocytes and protects cardiomyocytes from death at least in part through STAT3-induced

Original received October 12, 2005; final version accepted March 9, 2006.

From the Department of Cardiovascular Science and Medicine, Chiba University Graduate School of Medicine, Japan.

Correspondence to Issei Komuro, MD, PhD, Department of Cardiovascular Science and Medicine, Chiba University Graduate School of Medicine, 1-8-1 Inohana, Chuo-ku, Chiba 260-8670, Japan. E-mail komuro-ky@umin.ac.jp

© 2006 American Heart Association, Inc.

*Arterioscler Thromb Vasc Biol.* is available at <http://www.atvbaha.org>

DOI: 10.1161/01.ATV.0000219697.99134.10

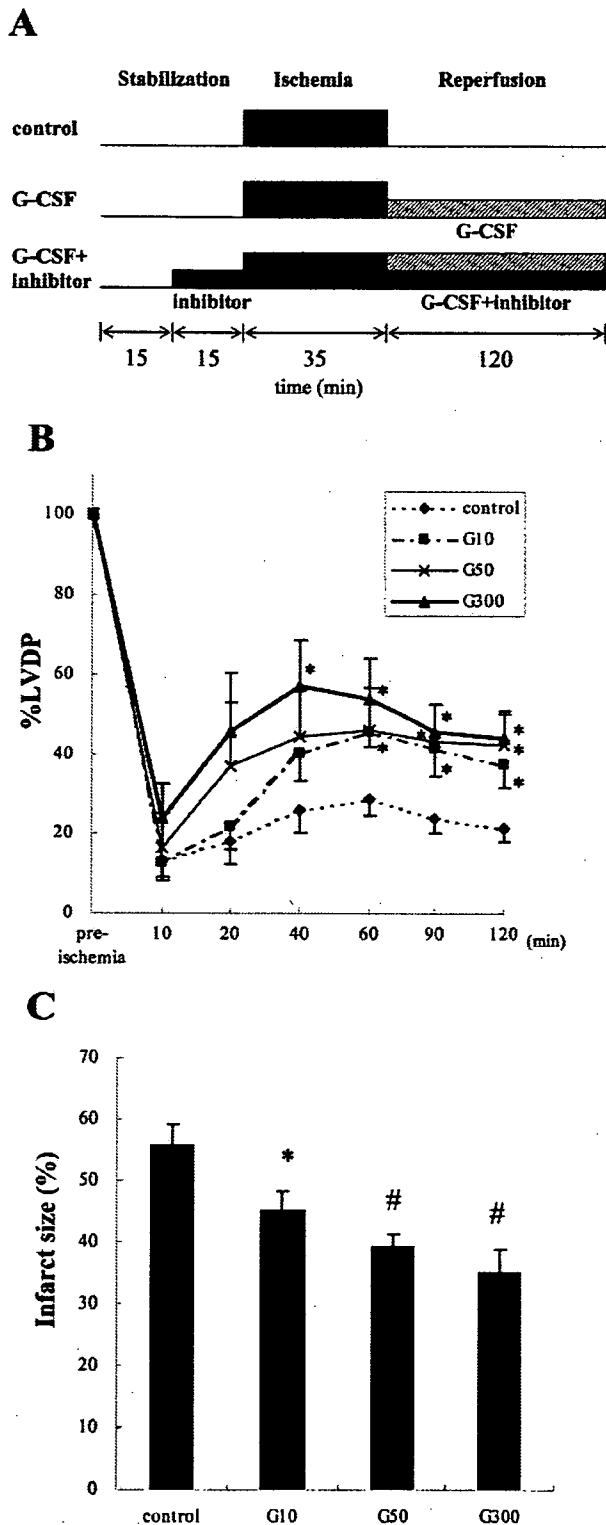


**Figure 1.** Protocol, LV pressure, and infarct size. **A**, Experimental protocol. **B**, %LVDP. Data shown indicate the mean percentage of LVDP recovery  $\pm$  SEM (each group  $n=6$ ). G10, G-CSF 10 ng/mL; G50, G-CSF 50 ng/mL; G300, G-CSF 300 ng/mL. \* $P<0.05$  vs control group. **C**, Infarct size. Results are given as mean  $\pm$  SEM (each group  $n=6$ ). G10, G-CSF 10 ng/mL; G50, G-CSF 50 ng/mL; G300, G-CSF 300 ng/mL. \* $P<0.05$  compared with control group. # $P<0.01$  compared with control group.

upregulation of antiapoptotic proteins.<sup>7</sup> Furthermore, pretreatment with G-CSF reduced myocardial IR injury using Langendorff perfusion model.<sup>7</sup> In that study, G-CSF was administered from 20 minutes before ischemia to 120 minutes after reperfusion to show the preconditioning effects of G-CSF on myocardium. Although the transcriptional regulation plays a critical role in preventing LV remodeling, G-CSF has acute, probably nongenomic effects on the heart.<sup>7</sup> In the present study, we therefore examined whether G-CSF has the postconditioning-like effects on myocardial IR injury using isolated perfused hearts and clarified the molecular mechanism.

## Materials and Methods

### Animals

Male Wistar rats ( $300 \pm 50$  g) were used for these studies. All animals were obtained from Takasugi Experimental Animals Supply Co Ltd, Japan. All experimental protocols were approved by the institutional animal care and use committee of Chiba University.

### Isolated Perfused Rat Heart

Hearts were excised rapidly and mounted on a Langendorff perfusion system. All isolated hearts were stabilized for 30 minutes by perfusion of Krebs-Henseleit (KH) buffer followed by 35 minutes of global normothermic ischemia and reperfusion (IR) for either 120 minutes to measure infarct size or 15 minutes to measure kinase activities as described previously.<sup>2</sup>

### Treatment Protocols

The experimental protocols for these studies are presented in Figure 1A. All the kinase inhibitors were dissolved in dimethyl sulfoxide (DMSO) and added to KH buffer so that the final DMSO concentration was  $<0.005\%$ . The hearts were randomly assigned to one of the following treatment groups: (1) administration of 0.005% DMSO vehicle (control group;  $n=5$ ); (2) administration of G-CSF (300 ng/mL) was started at the onset of reperfusion and continued throughout reperfusion (G-CSF group;  $n=5$ ); (3) G-CSF+Jak2 inhibitor AG490 (5  $\mu\text{mol/L}$ ; G+AG group;  $n=5$ ); (4) G-CSF+PI3K inhibitor LY294002 (5  $\mu\text{mol/L}$ ; G+LY group;  $n=5$ ); (5) G-CSF+mitogen-activated protein kinase kinase (MEK) inhibitor PD98059 (10  $\mu\text{mol/L}$ ; G+PD group;  $n=5$ ); (6) G-CSF+NO synthase (NOS) inhibitor *N*<sup>ω</sup>-nitro-L-arginine methyl ester (L-NAME; 30  $\mu\text{mol/L}$ ; G+L-NAME group;  $n=5$ ). The administration of each inhibitor was started 15 minutes before ischemia and continued throughout reperfusion. Additionally, hearts of 4 to 5 rats in each group were used to perform Western blot analysis, and hearts of 6 rats in each group were used to analyze the dose dependence of G-CSF-induced cardioprotection.

### LV Pressure

To evaluate the contractile function, a polyethylene film balloon was inserted into the cavity of the left ventricle through the left atrium. The balloon was filled with saline to adjust the baseline end-diastolic pressure to 5 to 10 mm Hg. LV pressure was measured continuously. LV developed pressure (LVDP) was designated as difference between systolic and diastolic pressures of LV. %LVDP represents percentage of LVDP recovery.

### Infarct Size

Hearts were sliced into 4 transverse sections and each was weighed, incubated for 3 minutes at 37°C in 1% triphenyltetrazolium chloride (TTC), and photographed, and the area of infarcted (unstained) and viable (stained) tissue was measured by computed planimetry. The mass-weighted average of ratio of infarct area to total cross-sectional area of LV from each slice was determined (% infarct size).



### Western Blot Analysis

At 15 minutes after reperfusion, the LV was excised and freeze-clamped in liquid nitrogen before being stored at  $-80^{\circ}\text{C}$ . We probed the membranes with antibodies to phospho-Jak2 (Tyrosine 1007/1008), phospho-STAT3 (Tyrosine 705), phospho-ERK (Threonine 202/Tyrosine 204), phospho-Akt (Serine 473), phospho-endothelial NOS (eNOS; phospho-eNOS; Serine 1177; Cell Signaling), Jak2, STAT3, Akt (Santa Cruz Biotechnology), ERK (Zymed Laboratories Inc), or eNOS (BD Biosciences). We used the enhanced chemiluminescence system (Amersham Biosciences Corp) for detection.

### Measurement of NO Release

A sealed reaction chamber was placed around the hearts to collect the effluent from perfused hearts by KH solution, and the chamber was filled with  $\text{N}_2$  gas and maintained at  $37^{\circ}\text{C}$ . In the bottom of chamber, the collecting space was placed and filled with the effluent, which was replaced continuously. NO release was measured using an NO-selective sensor (amiNO-700; Innovative Instruments Inc) as described previously.<sup>8</sup> The sensor was placed in the effluent to measure directly and quick NO concentration released from the hearts. The level of NO concentration (nmol/L) in the effluent was measured from preischemia throughout reperfusion. The sensor was calibrated by producing standard concentrations of NO based on dilutions of NO-equilibrated solutions (Innovative Instruments Inc). Data were digitally recorded and analyzed with APOLLO 4000 free radical analyzer (World Precision Instruments). NO concentration (% of preischemia) = NO concentration at each time after reperfusion (nmol/L)/NO concentration at preischemia (nmol/L)  $\times 100$  (%).

### Statistical Analysis

All data are presented as means  $\pm$  SEM. All data were analyzed by 1-way ANOVA followed by the Fisher procedure for comparison of means. A *P* value  $<0.05$  was considered statistically significant.

## Results

### G-CSF Protects Reperfused Myocardium

Isolated hearts were subjected to global ischemia for 35 minutes and then exposed to G-CSF during reperfusion. There was no difference in heart rate between control and G-CSF-treated groups. After reperfusion, LVDP was significantly higher in G-CSF-treated hearts than control hearts, and there was a dose dependency of G-CSF (Figure 1B). TTC staining revealed that infarct size was significantly reduced by G-CSF in a dose-dependent manner (control group  $55.8 \pm 3.2\%$  versus G-CSF 10 ng/mL;  $45.2 \pm 3.1\%$ , G-CSF 50 ng/mL;  $39.3 \pm 2.1\%$ , G-CSF 300 ng/mL,  $35.2 \pm 3.7\%$ ; Figure 1C).

### G-CSF Activates Various Signaling Pathways in Reperfused Myocardium

In the previous study, we demonstrated that cardiomyocytes have G-CSF receptors and that G-CSF activates Jak2, Akt, and ERK in cultured cardiomyocytes.<sup>7</sup> In this study, we examined whether the same signals were phosphorylated and activated by G-CSF in whole hearts during reperfusion. Western blot analysis using phosphoprotein-specific antibodies demonstrated that G-CSF (300 ng/mL) phosphorylated Jak2, STAT3, ERK, Akt, and eNOS as early as 7 minutes (data not shown), and the phosphorylation level reached a peak at 15 minutes (Figure 2A through 2E). Phosphorylation of the amino acid of each protein has been reported to associate with activation of each protein.

### Akt/eNOS Pathway Mediates G-CSF-Induced Cardioprotective Effects

To assess the signaling pathways involved in G-CSF-induced cardioprotection, hearts were treated with G-CSF in the presence of various inhibitors such as a MEK inhibitor PD98059, a Jak2 inhibitor AG490, a PI3K inhibitor LY294002, or a NOS inhibitor L-NAME. PD98059, AG490, and LY294002 completely inhibited G-CSF-induced phosphorylation of ERK, Jak2, and Akt, respectively (Figure 2A through 2E). Phosphorylation of eNOS by G-CSF was inhibited in the presence of AG490 or LY294002 but not PD98059 (Figure 2C). Furthermore, AG490 inhibited G-CSF-induced phosphorylation of Akt (Figure 2B).

To evaluate whether G-CSF increases NO production through eNOS phosphorylation, we measured NO concentration in the effluent by using an NO-selective sensor and its analyzer. NO concentration of the hearts was measured at the time of preischemia and 30 minutes after reperfusion. G-CSF (300 ng/mL) significantly increased NO production in the reperfused hearts (control group  $99.7 \pm 1.7\%$  versus G-CSF group  $109.1 \pm 2.0\%$ ;  $P < 0.05$ ; Figure 2F). The increase in NO production induced by G-CSF was suppressed completely by L-NAME (G+L-NAME group;  $96.6 \pm 1.0\%$ ; Figure 2F).

G-CSF-induced reduction in infarct size (control group  $55.8 \pm 3.2\%$ ; G-CSF group  $35.2 \pm 3.7\%$ ) was blocked by AG490 and LY294002 (G+AG group  $63.0 \pm 3.6\%$ ; G+LY group  $56.8 \pm 8.2\%$ ), whereas the pretreatment with PD98059 had no effect on G-CSF-induced reduction in infarct size ( $37.9 \pm 1.5\%$ ; Figure 3A and 3B). These results suggest that G-CSF protects the heart from IR injury by phosphorylating the Jak2-PI3K/Akt pathway but not the ERK pathway. To elucidate the downstream pathway of PI3K/Akt, we examined the role of eNOS using L-NAME. L-NAME treatment inhibited G-CSF-induced reduction in infarct size (G+L-NAME group  $52.4 \pm 6.9\%$ ; Figure 3A and 3B). Each inhibitor alone did not influence the infarct size (data not shown).

## Discussion

In the present study, we demonstrated that G-CSF has direct and acute protective effects on myocardium against IR injury by activating Akt-eNOS pathway in the isolated perfused rat hearts. Recently, G-CSF has been reported to prevent LV remodeling and dysfunction after acute MI in animal models.<sup>4-7</sup> Orlic et al reported that G-CSF induces myocardial regeneration by promoting mobilization of bone marrow stem cells into the injured region after MI.<sup>3</sup> However, recent studies demonstrated that bone marrow hematopoietic stem cells cannot transdifferentiate into cardiomyocytes in MI hearts.<sup>9,10</sup> We demonstrated recently that G-CSF acts directly on cardiomyocytes and induces the survival signals in post-MI hearts.<sup>7</sup> G-CSF-induced phosphorylation of Jak2-STAT3 pathway plays a critical role in upregulating the expression of antiapoptotic proteins and angiogenic factors on post-MI hearts. Although transcriptional regulation by STAT3 is important for preventing LV remodeling at chronic stage, Langendorff experiments revealed that other mechanisms may also be

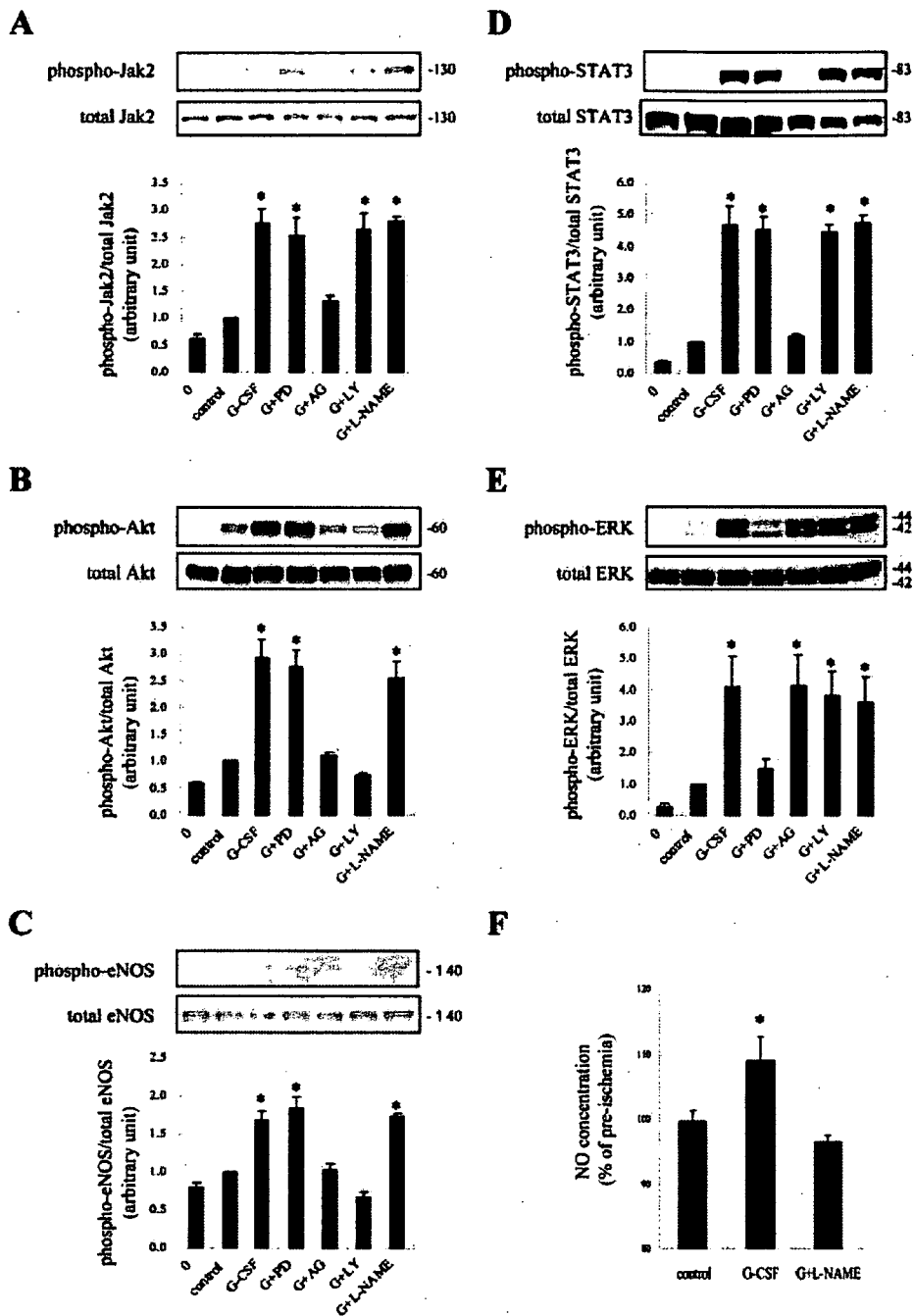


**Figure 2.** G-CSF-induced signaling pathway and involvement of G-CSF in NO production. A through E. Phosphorylation of various signal pathways in reperfused myocardium. Zero on the x axis indicates the onset of reperfusion. Results are given as means±SEM (each group n=4 to 5). G+PD, G-CSF+PD98059; G+AG, G-CSF+AG490; G+LY, G-CSF+LY294002; G+L-NAME, G-CSF+L-NAME. \**P*<0.05 compared with control group. Representative results of 5 independent experiments were shown. F, NO concentration (% of preischemia) at 30 minutes after reperfusion. Results are given as means±SEM (each group n=5). \**P*<0.05 compared with control group.

involved in the acute stage. G-CSF actually activated various signaling pathways such as Akt, ERK, and Jak2-STAT3 in cultured cardiomyocytes.<sup>7</sup>

In the present study, we examined whether G-CSF administered at the onset of reperfusion has acute postconditioning-like effects on myocardial IR injury. G-CSF phosphorylated and activated ERK, Jak2, STAT3,

Akt, and eNOS and significantly reduced the infarct size. Because Jak2 inhibitor AG490 inhibited G-CSF-induced phosphorylation of Jak2, STAT3, Akt, and eNOS but not ERK, and PI3K inhibitor LY294002 suppressed G-CSF-induced phosphorylation of Akt and eNOS but not Jak2, STAT3, and ERK, the signals are activated by the order of Jak2>PI3K>Akt>eNOS, and the signaling pathways of

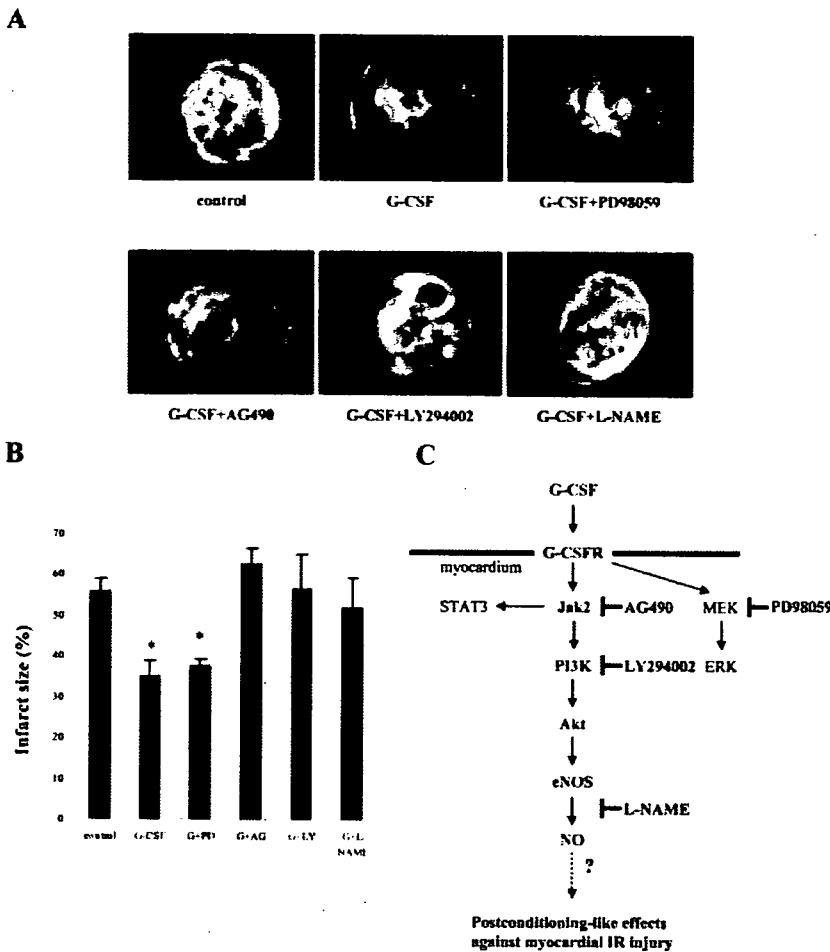


**Figure 3.** Signals in G-CSF-induced cardioprotection. A, TTC staining of hearts in each group (each group n=5). B, Infarct size. Results are given as means±SEM (each group n=5). G+PD, G-CSF+PD98059; G+AG, G-CSF+AG490; G+LY, G-CSF+LY294002; G+L-NAME, G-CSF+L-NAME. \*P<0.05 compared with control group. C, Hypothetical scheme postulating the possible signaling pathways induced by G-CSF.

ERK may be different. G-CSF increased NO production in reperfused hearts, and its effect was inhibited by L-NAME. Furthermore, the reduction of infarct size afforded by G-CSF administration was completely abolished in the presence of AG490, LY294002, and L-NAME but not PD98059. These results suggest that G-CSF acts directly on the myocardium during IR injury and has cardioprotective effects even if G-CSF administration is started after reperfusion, and that G-CSF-induced activation of Akt-eNOS and production of NO are important for its acute cardioprotective effects (Figure 3C).

Transcriptional regulation by the phosphorylation of Jak2-STAT3 pathway is one of the key mechanisms in G-CSF-mediated cardioprotection against MI heart in the chronic stage, whereas the Akt-eNOS pathway may be very important in the acute stage. eNOS has been reported to be phosphorylated by Akt, and activated eNOS-producing NO has been reported to play a pivotal role in the cardioprotection of preconditioning by preserving ischemic blood flow and attenuating platelet aggregation and neutrophil-endothelium interaction after IR.<sup>11</sup> NO is known to be the trigger for ischemic preconditioning, especially in the late phase of preconditioning, and to activate downstream pathways including protein kinase G, mitochondrial ATP-sensitive K<sup>+</sup> channels, free radicals,

and protein kinase C. However, it remains unknown whether NO acts as the trigger for postconditioning as well as preconditioning. It has been reported recently that postconditioning inhibits the opening of mitochondrial permeability transition pore (mPTP), which is involved in IR injury,<sup>12</sup> and that NO inhibits mPTP opening.<sup>11</sup> Because glycogen synthase kinase-3β, another downstream molecule of Akt, has been reported to induce opening mPTP,<sup>13</sup> glycogen synthase kinase-3β may also be involved in G-CSF-induced inhibition of IR injury. Further studies are needed to clarify the downstream of NO in the postconditioning-like effects of G-CSF against IR injury. The present study suggests that G-CSF can be used as a novel and valuable postconditioning agent.

### Acknowledgments

This work was supported by a grant-in-aid for scientific research, developmental scientific research, and scientific research on priority areas from the Ministry of Education, Science, Sports, and Culture and by the Program for Promotion of Fundamental Studies in Health Sciences of the Organization for Drug ADR Relief, R&D Promotion and Product Review of Japan. The authors thank E. Fujita, R. Kobayashi, M. Ikeda, Y. Ohtsuki, A. Furuyama, and M. Tamagawa for excellent technical assistance.

## References

- Vinten-Johansen J, Zhao ZQ, Zatta AJ, Kin H, Halkos ME, Kerendi F. Postconditioning—A new link in nature's armor against myocardial ischemia-reperfusion injury. *Basic Res Cardiol*. 2005;100:295–310.
- Tsang A, Hausenloy DJ, Mocanu MM, Yellon DM. Postconditioning: a form of "modified reperfusion" protects the myocardium by activating the phosphatidylinositol 3-kinase-Akt pathway. *Circ Res*. 2004;95:230–232.
- Orlic D, Kajstura J, Chimenti S, Limana F, Jakoniuk I, Quaini F, Nadal-Ginard B, Bodine DM, Leri A, Anversa P. Mobilized bone marrow cells repair the infarcted heart, improving function and survival. *Proc Natl Acad Sci U S A*. 2001;98:10344–10349.
- Ohtsuka M, Takano H, Zou Y, Toko H, Akazawa H, Qin Y, Suzuki M, Hasegawa H, Nakaya H, Komuro I. Cytokine therapy prevents left ventricular remodeling and dysfunction after myocardial infarction through neovascularization. *FASEB J*. 2004;18:851–853.
- Minatoguchi S, Takemura G, Chen XH, Wang N, Uno Y, Koda M, Arai M, Misao Y, Lu C, Suzuki K, Goto K, Komada A, Takahashi T, Kosai K, Fujiwara T, Fujiwara H. Acceleration of the healing process and myocardial regeneration may be important as a mechanism of improvement of cardiac function and remodeling by postinfarction granulocyte colony-stimulating factor treatment. *Circulation*. 2004;109:2572–2580.
- Iwanaga K, Takano H, Ohtsuka M, Hasegawa H, Zou Y, Qin Y, Odaka K, Hiroshima K, Tadokoro H, Komuro I. Effects of G-CSF on cardiac remodeling after acute myocardial infarction in swine. *Biochem Biophys Res Commun*. 2004;325:1353–1359.
- Harada M, Qin Y, Takano H, Minamino T, Zou Y, Toko H, Ohtsuka M, Matsuura K, Sano M, Nishi J, Iwanaga K, Akazawa H, Kunieda T, Zhu W, Hasegawa H, Kunisada K, Nagai T, Nakaya H, Yamauchi-Takahara K, Komuro I. G-CSF prevents cardiac remodeling after myocardial infarction by activating the Jak-Stat pathway in cardiomyocytes. *Nat Med*. 2005;11:305–311.
- McVeigh GE, Hamilton P, Wilson M, Hanratty CG, Leahey WJ, Devine AB, Morgan DG, Dixon LJ, McGrath LT. Platelet nitric oxide and superoxide release during the development of nitrate tolerance: effect of supplemental ascorbate. *Circulation*. 2002;106:208–213.
- Murry CE, Soonpaa MH, Reinecke H, Nakajima H, Nakajima HO, Rubart M, Pasumarthi KB, Virag JJ, Bartelmez SH, Poppa V, Bradford G, Dowell JD, Williams DA, Field LJ. Hematopoietic stem cells do not transdifferentiate into cardiac myocytes in myocardial infarcts. *Nature*. 2004;428:664–668.
- Balsam LB, Wagers AJ, Christensen JL, Kofidis T, Weissman IL, Robbins RC. Hematopoietic stem cells adopt mature hematopoietic fates in ischemic myocardium. *Nature*. 2004;428:668–673.
- Schulz R, Kelm M, Heusch G. Nitric oxide in myocardial ischemia/reperfusion injury. *Cardiovasc Res*. 2004;402–413.
- Argaud L, Gateau-Roesch O, Raïsky O, Loufouat J, Robert D, Ovize M. Postconditioning inhibits mitochondrial permeability transition. *Circulation*. 2005;111:194–197.
- Juhászova M, Zorov DB, Kim SH, Pepe S, Fu Q, Fishbein KW, Ziman BD, Wang S, Ytrehus K, Antos CL, Olson EN, Sollott SJ. Glycogen synthase kinase-3 $\beta$  mediates convergence of protection signaling to inhibit the mitochondrial permeability transition pore. *J Clin Invest*. 2004;113:1535–1549.